Isoteric vapor pressure

Temperature data for water sorption in hardened cement paste: enthalpy, entropy and sorption isotherms at different temperatures

Radjy, Fariborz; Sellevold, Erik J.; Hansen, Kurt Kielsgaard

Publication date:
2003

Document Version
Publisher's PDF, also known as Version of record

Fariborz Radjy
Erik J. Sellevold
Kurt Kielsgaard Hansen

ISOSTERIC VAPOR PRESSURE – TEMPERATURE DATA FOR WATER SORPTION IN HARDENED CEMENT PASTE:

ENTHALPY, ENTROPY AND SORPTION ISOTHERMS AT DIFFERENT TEMPERATURES

BYG·DTU

TECHNICAL
UNIVERSITY
OF DENMARK

Report
BYG·DTU R-057
2003
ISSN 1601-2917
ISBN 87-7877-118-8

ISOSTERIC VAPOR PRESSURE – TEMPERATURE DATA FOR WATER SORPTION IN HARDENED CEMENT PASTE: ENTHALPY, ENTROPY AND SORPTION ISOTHERMS AT DIFFERENT TEMPERATURES

Fariborz Radjy[1]
Erik J. Sellevold[2]
Kurt Kielsgaard Hansen[3]

BYG•DTU - Department of Civil Engineering
Brovej
DTU – Building 118
DK-2800 Kgs. Lyngby
Denmark

This report is available at:
www.byg.dtu.dk/publicering/rapporter/R-057.pdf

[1] At present: Managing Partner, Digital Site Systems, Pittsburgh, Pa, USA <fradjy@digitalsitesystems.com>
[2] At present: Professor of concrete technology at the Department of Structural Engineering, NTNU, Trondheim, Norway <erik.sellevold@bygg.ntnu.no>
[3] At present: Associate Professor, BYG•DTU <kkh@byg.dtu.dk>

FOREWORDS AND ACKNOWLEDGEMENTS

The Thermo Piestic Analysis system (the TPA-system) was designed and constructed by Fariborz Radjy at the Building Materials Laboratory (LBM), Technical University of Denmark (DTU) in the period 1968 – 1973. The TPA-system makes it possible to measure the absolute water vapour pressure exerted by a controlled amount of pore water in microporous materials as a function of temperature. The amount of pore water can vary from zero in a dry state to saturation. After calibration, a number of experiments were performed by F. Radjy on two hardened cement pastes and porous Vycor glass. The results were used to calculate a number of thermodynamic properties of the pore water. The TPA-system and the results were presented at two Annual Meetings of the American Ceramic Society; the 76th, Pittsburgh, May 1974 and the 77th, Washington DC, May 1975. No publication of record has been made, but the results have been presented orally several times at different meetings since then by the present authors. Based on the data an internal report [17] has been made where sorption isotherms over a wide range of temperatures were generated. In a PhD work [18] data for one of the steam cured hardened cement pastes has been used to calculate a number of thermodynamic parameters.

PART I of this report documenting the TPA-system is practically identical to the original manuscript (1975) by F. Radjy. PART II was written by Erik J. Sellevold in 2002 with editorial assistance from Kurt Kielsgaard Hansen. The results were generated using the original regression coefficients, and incorporating data on a room temperature cured hardened cement paste in addition to the original steam cured ones and the porous vycor glass. The "new" experiments were run by E. J. Sellevold in 1975 after F. Radjy had left Denmark. We gratefully acknowledge the contribution of Ulla Gjøl Jacobsen who did a large part of the experimental work, and of the head of the laboratory Professor Torben C. Hansen for his support of the project. The calculations, tables and figures in PART II were produced by MSc student Thomas Munch at DTU. We thank him for good work.

The financial support was given by the Danish Science Fund (STVF).

April 2003
Revised January 2004

Fariborz Radjy Erik J. Sellevold Kurt Kielsgaard Hansen

ABSTRACTS

PART I:
In order to generate isosteric (constant mass) vapor pressure – temperature data (P-T data) for adsorbed pore water in hydrated cement paste, the Thermo Piestic Analysis system (the TPA system) described herein was developed. The TPA system generates high precision equilibrium isosteric P-T data automatically during slow heating and cooling. The generated data are subjected to regression analysis leading to very close curve fitting of the P-T data and enabling appropriate enthalpy and entropy computations. The TPA system's absolute accuracy is checked by generating P-T data for pure water. The accuracies for pressure, enthalpy and entropy are found to be 0.5% or less.

PART II:
The TPA-system has been used to generate water vapor pressure – temperature data for room temperature – and steam cured hardened cement pastes as well as porous vycor glass. The moisture contents range from saturated to dry and the temperatures range from 2 to 95 °C, differing for the specimen types. The data has been analyzed to yield differential enthalpy and entropy of adsorption, as well as the dependence of the relative vapor pressure on temperature at various constant moisture contents. The implications for the coefficient of thermal expansion have been explored.

The main conclusions are:

Both enthalpy and entropy of adsorbed water in hardened cement paste and porous vycor glass decrease strongly with the relative vapor pressure exerted by the pore water. At saturation the values correspond to bulk water, reducing to values lower than for ice (extrapolated to 20 °C) in the relative vapor pressure range below about 30% for hardened cement paste cured at room temperature and about 10% for porous vycor glass.

Both enthalpy and entropy of adsorbed water decreases at any relative vapor pressure in the order:

Porous vycor glass
↓
Steam cured hardened cement paste
↓
Room temperature cured hardened cement paste

This implies fines pore structure and increasing influence of solid surface forces in the same order.

For a sample with fixed moisture content in equilibrium with a water vapor pressure less than saturation, a temperature increase results in an increase in the relative vapor pressure (relative humidity). This implies that the thermal expansion coefficient increases as the moisture content is reduced from saturation, since the relative humidity increase on heating produces swelling in addition to the pure thermal effect. The effect is quantified.

TABLE OF CONTENTS

LIST OF TABLES

LIST OF FIGURES

PART I: THE TPA SYSTEM AND METHODS OF DATA ANALYSIS

1. INTRODUCTION

During the years following the publication of PCA bulletin No. 22 [1] by Powers and Bownyard, the fundamental importance of pore structure and its interaction with water in hydrated cement paste (HCP) has become increasingly clearer and progressively more important [2]. Sorption thermodynamics, while not always applicable because of the basic irreversibilities of the system HCP-water, is nevertheless one of the few tools available for a fundamental elucidation of structure-property relationships in this engineering system. Yet, a literature review in 1968-69 showed a conspicuous lack of systematic thermodynamic data. It was with these thoughts that the project to be reported here on a somewhat delayed time scale was initiated in 1969.

The equipment development undertaken was in order to enable a direct measurement of sorption isosteres, i.e. vapor pressure versus temperature at constant moisture content in HCP. From the isosteres both such thermodynamic parameters as enthalpy and entropy of sorption can be computed directly, and sorption isotherms at different temperatures obtained indirectly. After approximately one year of work with an all glass manually operated system [3], it became evident that a high precision system with large, automatic data generation capability was necessary. It was thus after some three to four years of work that the system referred to herein as the Thermo Piestic Analysis system (the TPA system) was finally developed. As the name implies, the system measures pressure as a function of temperature while the sample is kept in an essentially closed isosteric condition. A detailed description of the TPA system, together with vapor pressure measurements performed with pure water as an overall check of the system is presented in PART I of the report. TPA results for hardened cement pastes and porous vycor glass are reported in PART II.

2. THE TPA SYSTEM

2.1 Principle of Operation

The sample is introduced into a vacuum system provided with direct water vapor pressure measurement capability and surrounded by a programmable thermostat. After appropriate treatment to induce equilibrium for the given moisture content, the sample is heated and cooled at sufficiently slow rates (usually 0.05 to 0.1 ºC/min) for dynamic equilibrium between preset temperature limits and both pressure and temperature are recorded digitally at close intervals on a data logger. At the conclusion of each heat/cool run, the moisture content of the sample is changed by distillation by either introducing (adsorption) a known amount of moisture into, or conversely withdrawing (desorption) a known amount from the sample. These processes are repeated until a set of adsorption and desorption isosteres are generated. The generated data are then analyzed and reorganized by using various computer programs.

2.2 Apparatus

The TPA system consists of four principal parts:

a. The vacuum system containing the pressure measuring head (transducer), the sample container inserted in a programmable precision thermostat, as well as the various auxiliary thermostats and vacuum pumps.

b. The sample programmable precision thermostat.

c. The pressure measuring system.

d. The data logging system.

2.2.1 The Vacuum System

A line diagram of the vacuum system is indicated in Fig. 1. The system, including the high vacuum valves, is all metal (SWAGE-LOCK system) except where marked "P" for o-ring connections to glass components. The metal tubing, valves and all connections at the various ports marked "P" in Fig. 1 are of standard 1/4 inch size. Under standard conditions (valve box at ~ 80 ºC, pressure measuring head at ~ 100 ºC), the leakage rate associated with the sample side was ~ 0.005 torr/hr. As indicated later, a procedure was developed for accurate leakage correction during data analysis.

The pressure measuring head (PMH) measures the pressure difference between the "zero" upper side connected to the vacuum pump system and the "active" lower side connected to the sample container. During normal operations, by closing the V2 valve, appropriately manipulating the ramaining valves, and continuously pumping on the zero side to maintain a low pressure of 10^{-5} torr, the PMH will directly measure the vapor pressure generated by the sample.

Normally the sample is loaded into the system in a pre-dried state, and after further drying in the apparatus, it is not removed from the system until a full set of sorption isosteres at different moisture contents are generated. The function of the capillary tube at port "P2" (CAP1) is to enable inducement of known changes in the moisture content by distillation of water between the sample container and the capillary tube. Initially it proved very difficult to collect the water in the capillary tube in a continous column. This problem was solved by inserting a small piece of magnetic metal inside the tube and moving this piece up and down with the aid of an external magnet. The amount of water entering or leaving the capillary tube (1.1 mm in diameter) is computed by monitoring the meniscus level using a travelling microscope having a resolution of 0.01 mm. In this manner a resolution of approximately 0.03 mg for moisture content changes could be obtained.

Introduction of properly de-aired water into the system met with many initial difficulties. The function of the reservoir R1 and the tube CAP2 next to the valve V5 is to enable production of thoroughly de-aired water for eventual introduction into the system. After the initial pump down, the water in R1 will be frozen and evacuated, then allowed to melt and distilled into a similar reservoir attached at the position of CAP2, and again frozen and evacuated. This process of distillation/freezing/evacuation is repeated about 6 or 7 times. Eventually the reserve capillary tube (CAP2) would be charged with water by distillation and substituted instead of CAP1 when needed.

The sample container "S" is illustrated in Fig. 2. The main body of the container is cylindrical with a somewhat skewed central, through tube. This tube is for insertion of a precision platinum resistance thermometer for measuring the specimen temperature. After inserting into the block thermostat, approximately 100 mm of the sample container would be within the thermostat well, and some 5 mm of the top would be taken up by the o-ring connection into the vacuum system. A specially constructed low power heater was mounted around the remaining (~ 65 mm) exposed part of the sample container. The neck heater was controlled by a differential controller set to a temperature differential of 15 ºC between the middle of the neck and the aluminium block (Al-block) wall. The controller was actuated by a differential thermocouple. During normal operation, the well in the Al-

block would be charged with sufficient mercury so that when the sample container is inserted into the well it would be fully surrounded and covered (~ 10 mm above the top surface) by mercury. For safety reasons, the mercury was topped by ~ 20 mm of silicone oil.

As indicated in Fig. 1, the main body of the vacuum system and the pressure measuring head are thermostated separately. The valves and the tubings are surrounded by a demountable, insulated copper box, heated by asbestos heating bands and thermostatically controlled at 80 ºC. The pressure measuring head is kept at approximately 100 ºC by an Al-jacket heater controlled by a proportional heater.

2.2.2 The Sample Thermostat

The sample thermostat surrounding the glass sample container "S" is a cylindrical aluminium block measuring 75 x 120 mm (diameter x height). The aluminium block contains a circular well (25 mm in diameter x 100 mm deep), in which the sample container is located such as to almost touch the well bottom. The block is heated by patch heaters in uniform intimate contact with the block vertical surfaces by being sandwich between the block and another Al-cylinder of 5 mm wall thickness. Cooling is provided by circulating cooling fluid through a thin-walled annular stainless steel cylinder in point contact with the Al-block assembly. This design enabled smooth attenuated cooling while providing the system with excellent thermal response time.

Two symmetrically located 100 ohm platinum resistance transducers (RTD) are located close to the sample well, one RTD being used for control purposes and the other for block temperature measurements. The aluminium block assembly is suspended inside a somewhat larger stainless steel container. At almost all points of contact between the stainless steel jacket and the Al-block low conductivity materials such as teflon plates and viton o-rings are used. Special precautions are taken regarding the thermostat's surface in order to minimize heat losses and thus reduce temperature gradients within the spcimen well. The whole Al-block/stainless steel jacket assembly is fully insulated, fixed on a jack capable of approximately 200 mm vertical motion, and connected to a precision temperature programmer as well as a low temperature (-40 ºC) bath for circulating cooling fluid through the Al-block thermostat.

The coolant flow is controlled by a solenoid valve commanded by a differential controller. The differential controller is actuated by a differential thermocouple measuring the temperature difference between the coolant inlet tube and the Al-block. During programmed heating and cooling or isothermal operation, the coolant differential controller is preset at an optimum temperature difference level for the given cooling/heating rate. This method of control has the two following advantages that 1) minimum internal temperature gradients consistent with the desired temperature change rates are generated, 2) the coolant circulation is automatically terminated for significantly higher than the room temperature operations. Typically the set coolant temperature differential was about 10 ºC for a programmed rate of about 0.05 ºC/min, and 30 ºC for 0.1 ºC/min.

The programable precision controller is contiously adjustable over a total temperature range of 110 ºC at rates from 0.002 to 4 ºC/min, and can maintain isothermal conditions at the upper and lower temperature limits for up to 27 hours. The overall system temperature range is in principle from -60 ºC to +170 ºC, although the maiximum actual limits used were -20 ºC and +150 ^{o}C, with normal operation within the range -10 ^{o}C to +110 ^{o}C.

2.2.3 The Pressure Measuring System

The MKS Baratron series 90 high precision pressure measuring system consists of the differential pressure measuring head (300 torr type) connected through a preamplifier to the Baratron pressure meter. The system has 8 full scale ranges (0.1, 0.3, 1, 3, 10, 30, 100, 300 torr), and read out either by an unbalanced mV output, or via the four decade switches to five digit resolution in the balanced mode. According to the manufacturer [4]: "True total pressure or vacuum measurements - independent of gas nature or composition - are obtained by electronically monitoring the physical displacements of a tensioned variable capacitance membrane". The pressure measuring head has an all-welded construction utilizing only metal and ceramic materials.

For the balanced mode of operation, a calibration table is supplied with error values ranging from 0 to about 2% of the reading. According to the manufacturer [5] the accuracy using the decade digital readout, and with reference to the calibration chart furnished, is 0.02% of full range plus 0.05% of the digital reading. Since during routine automatic runs it was anticipated that the pressure change could range up to 2 to 3 decades, an auto-ranging facility was added to the instrument. Based on the unbalanced mV signal, a motor coupled to the range switch would be actuated for a "down" or an "up" switch. It was thus always possible to maintain the output signal within 30% to 95% of the full scale and utilize the instrument optimally.

2.2.4 The Data Logging System

A 20 channel data logger (Consolidated Controls Corporation, USA) including the functions time, temperature (100 ohm Pt sensor) and mV was utilized. The data could be printed as well as punched on paper tape. The reading frequency could be adjusted from about every minute to every few hours. Independent span and zero adjustments could be performed for the various functions.

3. CALIBRATION

The MKS pressure measurements have their highest accuracy (0.1% full scale) when obtained from a balanced readout. However, for automatic data acquisition it is easiest and most practical to record the unbalanced mV directly, reducing the accuracy to 1 to 3%. This problem was overcome by generating various pressures within the TPA system using N_2 gas and recording the unbalanced mV versus the true pressure obtained using balanced mode decade switch and the manufacturer's corrections. The unbalanced mV's were measured on the data logger with an uncertainty of 0.01 mV. The mV range of the data logger was itself calibrated using a Leeds and Northrop potentiometer. For each range this process was repeated from 0 to 95 mV at 5 mV intervals, and for the given pressure value the mV signals on all the possible ranges were recorded. This method of data recording ensures that the results of calibration analysis will be such that for a given pressure the mV signals generated on two different ranges will be consistent with one another. The data thus generated for each range was subject to regression analysis with a "true torr" as the dependent and different combinations of x (= mV), x^2, x^3, $\sqrt{x}$, 1ogx as independents. For each range the combination of x-functions giving the best fit was selected as standard and built into various TPA computer programs. The standard deviation due to deviations from the best regression line as a percent of range varied from 0.06% (300 torr) to 0.5% (1 torr). Due to the low pressures involved, the two most sensitive ranges (0.1 and 0.3 torr) could not be calibrated as above, but were calibrated against the regression lines of the adjacent ranges.

The specimen temperature was measured by a Pt resistance thermometer integral with the data logger. The temperature calibration was performed by insertion in an intimate mixture of ice and destilled water for the zero setting of the data logger signal conditioner, while the span adjustment was performed by inserting the sensor into rigorously stirred boiling water. Due note was taken of the barometric correction which at the time turned out to be negligible. Although the temperature resolution was 0.01 ºC, the repeatability was approximately ±0.05 ºC.

A further calibration performed was to account for the dead volume correction associated with the sample side of the vacuum system. The specimen can exert different vapor pressures as the temperature is changed by exchanging moisture with its environment. If this moisture exchange is large, both the time to equilibrium will be increased and the isosteric condition violated. For the imposed standard isothermal conditions of the valve box at 80 ºC and the pressure measuring head at 100 ºC, the amount of water vapor in the sample side dead volume will be only a function of pressure. Using N_2 gas and with glass containers of known volumes attached at P1 and P2 in Fig. 1, the dead volume correction was found equal to 0.0345 mg/torr. This correction too was built into the data analysis programs. Its effect on the isosteric condition was generally found to be negligible.

4. EXPERIMENTAL PROCEDURE AND DATA ANALYSIS

4.1 Experimental Procedure

The general experimental procedure for operating the TPA system is somewhat as follows, the specific details naturally being dependent on the sample type. Normally a pre-dried sample is loaded into the apparatus and dried there in a standard manner before a number of adsorption and then desorption isosteres would be generated. At the end of the last desorption step, the sample would be weighed and the initial exact dry weight back calculated.

As indicated earlier, the vacuum system (specimen side) has a leakage rate ~ 0.005 torr/hr. An essential step in the operation of the TPA system is a specially developed degassing procedure enabling:

1) The removal of leaked air without disturbing the specimen's moisture state
2) Obtaining a good estimate of the leakage for a given heat/cool equilibrium run in order to compensate the recorded pressure data for leakage effect.

The procedure is performed at the end of an equilibrium heat/cool run and prior to changing the specimen moisture content for the next run. The principle involved is (with V2 closed, Fig. 1) to introduce sufficient water vapor into the zero side of the vacuum system such that the indicated pressure differential is the estimated pressure increase due to leakage. Now by closing V1 and opening V2, a gas/vapor redistribution between the zero and the specimen sides will occur. Due to the volume ratios involved, each degassing operation reduces the partial pressure of the leakage gasses by approximately one order of magnitude. The degassing operation was usually repeated four times. By comparing the pressure readings before and after degassing and noting the time since the last degassing, the actual leakage rate for each run is estimated and the recorded pressure data duly compensated for leakage.

The recorded data the for steam cured (97 ºC) HCP and the Porous Vycor Glass (PVG) samples were obtained during "equilibrium" heat/cool runs involving isothermal periods of few hours to one or two days at the upper and lower temperature limits. The rates used were of the order of 0.05 to 0.1

ºC/min between temperature limits within the range 0 to 95 ºC. Each equilibrium heat/cool run would usually take from about 30 to 72 hours. Due to the nature of the moisture exchanges involved for the generation of the isosteric P-T curves, lack of equilibrium would be reflected in heat/cool hysteresis with the cooling P-T curve lying above the corresponding heating curve. Therefore, coincidence of the heat/cool isosteres would incidate equilibrium. After much trial and error it was found that equilibrium could be approached closely if at each new moisture content the equilibrium run is preceded by a rapid (2 ºC/min) "equilibration" run with a 4 to 12 hour isothermal period at the maximum temperature limit. This rapid heat/cool run appears to ensure a uniform internal moisture distribution prior to final measurements.

For the room temperature cured HCP a different procedure was followed to be described in Part II.

4.2 Data Analysis

The recorded paper punched data, usually obtained at 1 ºC intervals, were screened for misreadings, reorganized, subjected to the various corrections discussed above and finally analyzed by regression by using a number of computer programs, some specially developed and some from the IBM standard library.

For comparison, and some computational reasons the corresponding P-T and thermodynamic data of liquid and solid (ice) water were built into the computer programs. The final printouts were organized in two different forms: 1) isosteric P-T data based on the best regression lines at close temperature intervals including the enthalpy and entropy thermodynamic parameters, as well as the corresponding bulk water data, 2) sorption isotherms at a number of selected temperatures.

The multiple linear regression analyses were performed with lnP (=y) as the dependent variable, while different combinations of the three variables T, 1000/T and lnT were in turn selected as the independents. An indication of the goodness of fit of the generated data for six different, typical cases are included in Table 1. The first four selections are seen to fit the data with almost equal accuracy. However, apart from the goodness of fit, the comparative behaviour of the regression lines in the extrapolated range must also be considered so that slopes and curvatures are always reasonable.

These considerations led to the choice of selection 4 as the standard form of the isosteric regression equation:

$$\ln P = A + B \cdot \frac{1000}{T} + C \cdot \ln T \qquad (1)$$

where A, B and C are moisture content dependent regression coefficients.

Due to the general characteristics of the system and based on many types of different observations, it was felt that the absolute accuracy associated with pressure measurements was higher than those for temperature. For instance one temperature uncertainty associated with the fact that the Pt-resistance sensor is not in direct contact with the specimen (see Fig. 2). In order to account for this possible discrepancy for each series of P-T isosteres the saturation isostere was compared to the P-T relationship for pure water [6] and temperature corrections computed for a perfect match of the two isosteres at all points. The computed temperature corrections were then applied to all isosteres generated over the full range of moisture contents. These temperature corrections were generally found to be between 0 and 0.3 ºC, and having negligible effects on the computed enthalpy and

entropy values. Thus even though the form of eq. (1) implies that T is measured with absolute accuracy and P fitted, by utilizing the internal reference procedure outlined, the accuracy of P-measurements was giving a greater weight.

On the basis of eq. (1) and using standard thermodynamic procedures [7], we obtain

$$\Delta h_{st}^{o} = h^{og} - h^{\sigma} = -R \cdot \left(\frac{d \ln P^{g}}{d(1/T)}\right) = -1000 \cdot R \cdot B + R \cdot C \cdot T \qquad (2)$$

and

$$\Delta s_{st}^{o} = s^{og} - s^{\sigma} = R \cdot \left(\frac{d \ln P^{g}}{d \ln T}\right) + R \cdot \ln\left(\frac{P^{g}}{P^{og}}\right) = R \cdot C + R \cdot \ln\left(\frac{P^{g}}{P^{og}}\right) - \frac{1000 \cdot R \cdot B}{T} \qquad (3)$$

where in the derivation of the above equations the water vapor phase has been treated as an ideal gas, and

$\Delta h_{st}^{o}, \Delta s_{st}^{o}$ = isosteric enthalpy and entropy of sorption relative to the saturated vapor state (superscript "o"), respectively

h^{og}, s^{og} = water vapor enthalpy and entropy at the saturation vapor pressure, respectively

h^{σ}, s^{σ} = absorbed water differential enthalpy and entropy, respectively

P^{g}, P^{og} = water vapor pressure and saturation vapor pressure, respectively

R = gas constant

T = absolute temperature

All units being in calorie, mole, K combinations.

As a consequence of the assumed ideal gas behaviour the parameters h^{g} and h^{og}, and consequently Δh_{st}^{o} and Δh_{st} are identical.

5. CHECK OF THE SYSTEM VERSUS PURE WATER

In order to obtain overall estimates of the accuracies for the measured and computed parameters, two complete sets of experiments were performed on pure water and the results compared to the corresponding published standard data [6]. Carefully de-aired water was distilled into the sample container "S" of Fig. 1 which had been previously filled with glass balls. The glass balls were introduced so that the thermal properties would be somewhat similar to the actual test conditions when the container would be loaded with a porous powder. The water sample was subjected to two sets of measurements at 0.05 and 0.1 ºC/min. The operation of the apparatus and the data analysis were in accordance with the standard procedures previously described. The temperature range covered was from 0.7 to 74 ºC.

Since the results obtained at the two temperature rates matched very closely, only the measurements performed at 0.05 ºC/min will be discussed here.

A sample of the generated P-T data at 10 ºC intervals (actual measurements were performed every 1 ºC) together with the computed thermodynamic parameters are compared with the standard water data [6] in Table 2. The reported experimental P-T values are based on the regression line fully detailed in Table 3. The computation of the enthalpies and entropies of condensation were in accordance with equations analogous to eqs. (2) and (3) but taking due account of the slight non-ideality of water vapor by including influences due to the second and third virial coefficients [6]. The standard data included in Table 2, and indeed build into the system of computer programs, were generated from the P-T regression line given by Baine [6]. Again the enthalpy and entropy computations were performed with due regard for the second and third virial coefficients. As it is evident from Table 2, the measured and the standard data match very closely. This close matching is true for all the three sets of data identified by "Heat", "Cool", and "Cool/Heat".

An estimate of the system accuracy may be obtained by computing the standard deviation of the differences between the measured and the standard values for each parameter shown in Table 2, for the full range of the data. In order to obtain standard deviations as a percent of the measured values at each points, actually the computations were performed by obtaining the standard deviations of the differences of the natural logarithms of the corresponding parameters. These computations for the "Heat" series resulted in the standard deviation error estimates for $\delta P/P$, $\delta \Delta h/\Delta h$ and $\delta \Delta s/\Delta s$ of 0.4%, 0.5% and 0.5%, respectively, where % refers to the standard deviation (δ) of the differences between measured and standard values expressed as % of parameter value. At a later stage in the experimental work, similar analyses of saturation P-T data generated by samples of hydrated cement paste and porous vycor glass lead to error estimates of the order of 0.3% to 0.5%.

6. CONCLUSION

The Thermo Plastic Analysis system (TPA system) developed for automatic generation of high precision P-T data is seen to be capable of operating within the temperature range from -10 to +100 ºC and pressure range from 10^{-2} to 300 torr at absolute accuracies of 0.5% or less. The system credibility and accuracy is established by generating P-T data for pure water and comparison with standard data. Accordingly, the basis for utilizing the system for moisture adsorbing systems is established.

TABLE 1. Regression selections, variables, and standard deviations as % of P.

Y=ln P						HCP		
Selection				Water	Water	Dry	Semi Wet	Wet
No.	T	1000/T	ln T	(0.05)*	(0.10)*	(0.05)*	(0.05)*	(0.05)*
1	X	X	X	0.58	0.29	0.55	0.53	0.41
2	X	X		0.61	0.29	0.61	0.53	0.46
3	X		X	0.68	0.32	0.61	0.53	0.55
4		X	X	0.60	0.30	0.61	0.53	0.45
5		X		1.02	1.40	0.77	1.27	1.04
6			X	4.47	4.95	0.67	4.81	4.40

* During heating at indicated rates (^{o}C/min).

TABLE 2. Comparison of measured and standard values for pure water heated and cooled at 0.05 ºC/min.

Pressure [Torr]				Enthalpy [kcal/mole]		Entropy [kcal/mole/ºC]	
T[ºC]	T-PROG	Measured	Standard	Measured	Standard	Measured	Standard
0	CH*	4.629	4.581	10.67	10.76	39.05	39.41
	HEAT	4.632		10.66		39.02	
	COOL	4.635		10.67		39.05	
10	CH	9.254	9.205	10.58	10.66	37.38	37.65
	HEAT	9.255		10.58		37.36	
	COOL	9.264		10.58		37.37	
20	CH	17.56	17.53	10.50	10.56	35.82	36.02
	HEAT	17.56		10.50		35.80	
	COOL	17.58		10.50		35.80	
30	CH	31.81	31.82	10.41	10.46	34.35	34.50
	HEAT	31.80		10.41		34.35	
	COOL	31.83		10.41		34.34	
40	CH	55.22	55.32	10.33	10.36	32.97	33.07
	HEAT	55.20		10.33		32.98	
	COOL	55.25		10.32		32.96	
50	CH	92.29	92.52	10.23	10.25	31.66	31.72
	HEAT	92.28		10.24		31.67	
	COOL	92.31		10.23		31.64	
60	CH	149.0	149.4	10.14	10.15	30.42	30.45
	HEAT	149.0		10.14		10.44	
	COOL	149.0		10.13		30.40	
70	CH	233.1	233.7	10.04	10.04	29.24	29.26
	HEAT	233.2		10.04		29.27	
	COOL	233.0		10.03		29.22	
80**	CH	354.5	355.2	9.932	9.931	28.12	28.12
	HEAT	354.7		9.942		28.15	
	COOL	354.2		9.923		28.10	
90**	CH	525.0	525.9	9.825	9.822	27.05	27.05
	HEAT	525.6		9.838		27.09	
	COOL	524.3		9.815		27.03	

* Values based on regression analysis of mixed Cool/Heat data.

** Extrapolated outside the measured range of 0.7 to 74 ^{o}C.

TABLE 3. Experimental P-T regression line for pure water (0.05 ^{o}C/min).

$$Y = \ln P = A + B \cdot \frac{1000}{T} + C \cdot \ln T$$

	N	A	B	C	STD DEV as % of P
CH	141	47.730	-6.4733	-4.0105	0.51%
STD DEV			0.0629	0.2026	
HEAT	87	46.928	-6.4366	-3.8915	0.60%
STD DEV			0.0957	0.3065	
COOL	52	48.050	-6.4858	-4.0592	0.31%
STD DEV			0.1978	0.6099	

N = Number of measurements analyzed by regression.
CH = Cool/Heat data treated as one set.

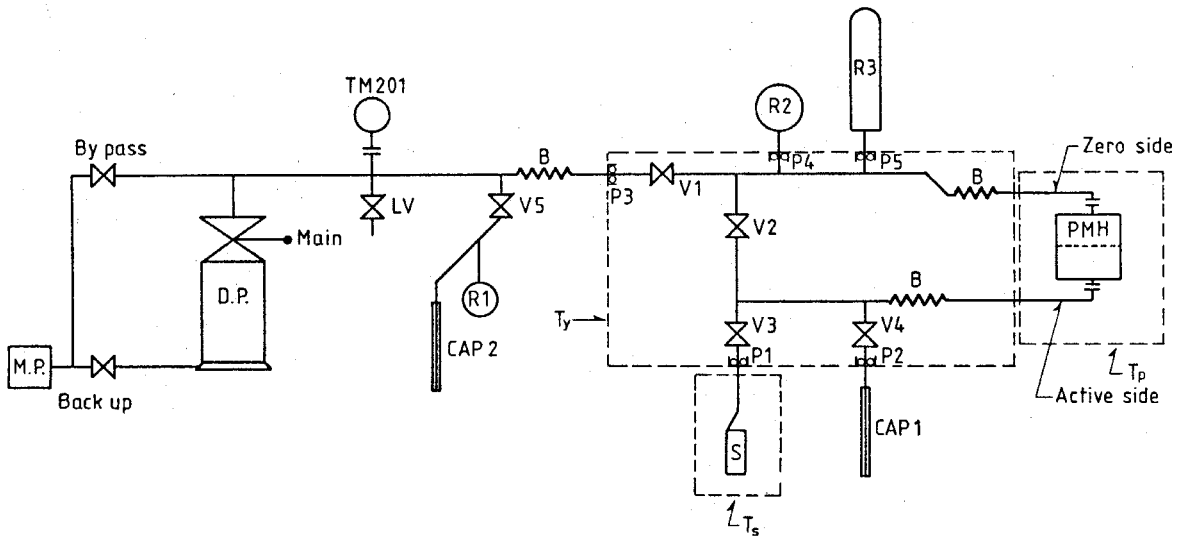

M.P. = mechanical pump
D.P. = diffusion pump
LV = leak valve
CAP = capillary tube (1.1 mm) for water
V = valve
R = glass reservoirs
B = flexible steel bellows
P = o-ring connections
S = specimen container
PMH = pressure measuring head
TM201 = Leybold pressure gage
T_s = temperature T_s
T_y = temperature T_y
T_p = temperature T_p

Dotted lines indicate thermostated regions.

Fig. 1. The Thermo Piestic Analysis system (the TPA system)

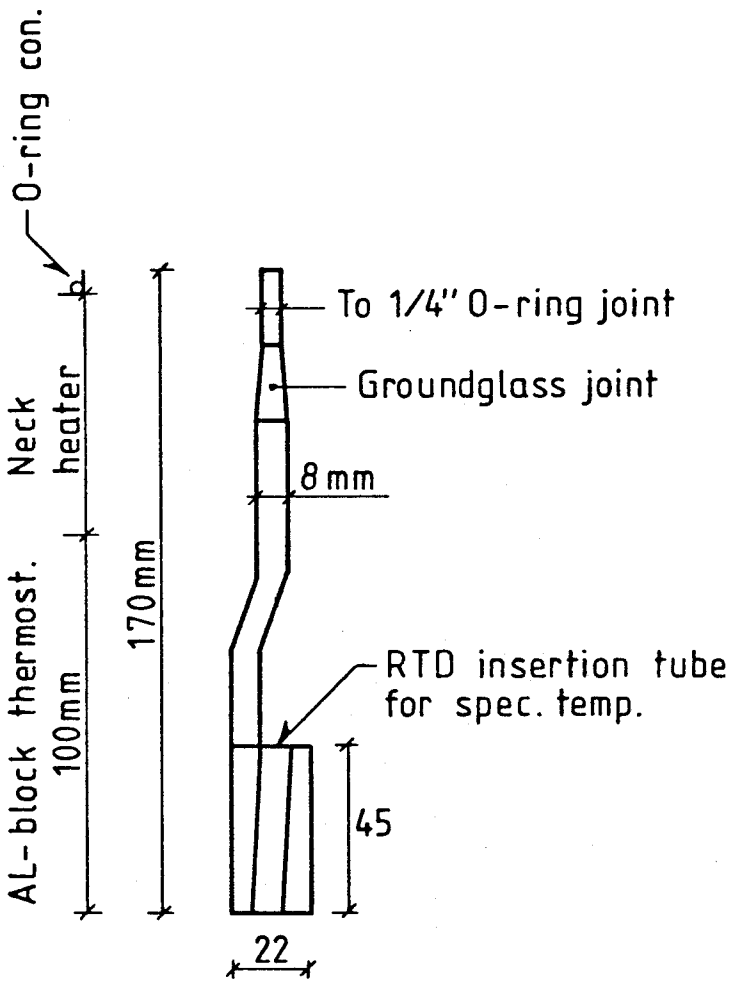

Fig. 2. The sample container “S”.

PART II: DATA FOR HARDENED CEMENT PASTE AND POROUS VYCOR GLASS

1. EXPERIMENTAL PROGRAM

The Thermo Piestic Analysis system (the TPA system) and procedures described in Part I of this report were applied to water sorption in two HCP's cured at 97 ºC (HCP35ST, HCP45ST), one cured at room temperature (HCP50RT) and PVG according to the program shown in Table 4.

TABLE 4. Experimental conditions.

		HCP35ST$^+$	HCP45ST$^+$	HCP50RT$^+$	PVG
Number of steps:					
Adsorption (ADS)		20	17	-	15
Desorption (DES)		10	-	17	10
Range of water	LOW	0/9.0*	14.8	98.0	0/29.2*
content (mg/g_{dry})	HIGH	179.7	136.1	320.3	227.8
Range of vapor	LOW	0.0/0.001*	0.003	0.261	0.001/0.217*
pressure (P/P_0)	HIGH	1.00	0.982	0.993	1.00
TPA system	LOW	2	2	5	25
T-range (ºC)	HIGH	95	80	30	70
Rate of T-change (ºC/hr)		3	3	1.2	6

$^+$ The number in the specimen identification refers to the w/c-ratio in %.
* The first number refers to condition at start of adsorption, the second at end of desorption.

The two steam cured HCP and the PVG samples were dried before TPA testing, which included first adsorption, then desorption steps. Steam curing was used in order to obtain a stable structure w.r.t. the applied temperature range (TABLE 4). The room temperature cured HCP has a structure unstable both with respect to temperature and moisture variations. This sample was therefore only tested during first desorption, in steps from a near saturated state (after nearly 3 years water curing) and in the moderate temperature range 5 to 30 ºC at each desorption step.

2. MATERIALS AND PROCEDURES

The cement from Aalborg Portland was the RAPID type with calculated compound composition as follows: C_3S = 66%, C_2S = 12%, C_3A = 8%, C_4AF = 6% and $C\bar{S}$ = 4.3%. The Blaine fineness was 336 m^2/kg.

The pastes were mixed in a vacuum mixer at the w/c-ratios 0.35 (HCP35ST), 0.45 (HCP45ST) and 0.50 (HCP50RT), and moulded in teflon tubes. The tubes with ST samples were heated to 97 ºC in steam for 3 hours, kept there until demoulding after 1 day and then steam cured for an additional 9 days, after which the samples were stored in water for about 2 years at room temperature. Properties of such steam cured cement pastes have been reported previously [8, 9, 10]. The RT sample was stored for 1 day in the mould at room temperature, then demoulded and cured in water for nearly 3 years before testing.

Porous vycor Glass (PVG) has been used extensively as a model material for HCP. It has a porosity of about 33 Vol.-%, with a narrow pore size distribution around 4 nm equivalent radius. In contrast to HCP its water sorption characteristics are reproducible from one sorption cycle to

the next. Some materials properties for the particular glass used here are given in [11].

The ST-TPA specimens were in powder form with particle sizes between 50 and 150 μm. The specimens were crushed and sieved in a glove box, and then P-dried (vapor pressure $8 \cdot 10^{-3}$ torr at 20 ºC) in a desiccator 4 months before being placed in the TPA cell. HCP50RT was crushed under water to a size range 125 to 250 μm. Specimen weights were about 8 g.

The heating and cooling rates were 3 ºC/hr for ST-HCP and 6 ºC/hr for PVG since the later requires less time for vapor pressure equilibrium. The rates and times spent isothermally before and after tests were determined by pilot runs. The criteria were, as already discussed in Part I, that the vapor pressure at the same isothermal temperature before and after an isosteric run were close to the same, and that the heat-cool hysteresis was acceptable, i.e. that it was practically invisible in the control plots. Thermodynamic data calculated from heat and cool separately will be given, and these of course provide the final test of experimental accuracy. The above remarks and procedures do not apply to the HCP cured at room temperature. The time to equilibrium was longer as evidenced by the systematic heat-cool hysteresis, compare Tables 6 and 7. After crushing under water the HCP50RT powder was placed in a desiccator at $P/P^o = 0.97$ for about 5 months before starting the TPA tests. After each moisture change step there was an isothermal waiting period of at least one day before the heat-cool cycle was started, but no quick heat-cool treatment was imposed as for the other samples. Generally only heat data are available for HCP50RT, but some data sets from both heat and cool will be given separately to indicate the magnitude of the hysteresis effect.

3. RESULTS AND DISCUSSION

3.1 Drying Procedure

The drying condition of 105 °C and 4.6 torr vapor pressure was chosen for convenience. Fig. 3 shows drying isosteres for two samples in the T-range from 25 to 105 °C plottet from the regression analysis of the experimental data. A curve for P-drying with the condition $8 \cdot 10^{-3}$ torr at 25 °C is plottet parallel to the others for reference; as is seen, the P-drying condition corresponds to about 3 torr at 105 °C, i.e. quite close to the chosen one of 4.6 torr (vapor pressure of water at 0 °C).

3.2 Sorption Isotherms at 20 °C

Fig. 4 shows all the measured sorption isotherms at 20 °C, using the regression analysis of the experimental data. The PVG curves (adsorption and desorption) demonstrate the very narrow pore size range of the material, most of the pores empty around $P/P^o = 0.70$, corresponding to a meniscus radius of about 3.5 nm according to the Kelvin equation. There is little hysteresis below $P/P^o = 0.6$ and above 0.8. Of the HCP samples only HCP35ST has both adsorption and desorption curves. There is significant hysteresis, however note that a large part is caused by "zero hysteresis", i.e. the irreversibility of the dry weight in the standard dry state. The dry weight after the desorption was 9 mg/g_{dry} higher than after first drying, see later tabulated values.

The saturation moisture contents need to be remarked. HCP50RT shows a value of 0.32 g/g_{dry} which was measured by weighing in the initial state ($P/P^o = 0.97$) and in the final dry state. Chunk specimens of the same parent material gave a value of 0.29 g/g_{dry} from a saturated state after 3 years water storage (as marked in Fig. 4) It therefore seems that the chosen powder

fraction (0.125 – 0.250 mm) is more porous than the HCP as a whole. The value of 0.29 corresponds exactly to the expected (calculated) one, based on a chemical shrinkage of 25.4% for the chemically bound water, and the measured amount of chemically bound water of 0.20 g/g_{ign}. The equation used for the calculation is:

$$\varepsilon_T = \frac{v/c - 0.746 \cdot w_n}{1 + w_n} \; g/g_{dry}.$$

For the two steam cured HCP the expected saturation values were 0.26 g/g_{dry} for HCP45ST (actually measured on chunks to be the same), and 0.20 g/g_{dry} for HCP35ST; both values marked in Fig. 4. Neither sample was conditioned to such high water content in the TPA adsorption runs (see Fig. 4) since the vapor pressure data showed that liquid water values were reached at lower moisture contents, presumably because of the coarse porestructures of steam cured HCP.

Only HCP50RT was measured in the TPA system during first desorption. Even so, it behaves very differently from HCP35ST during second desorption. In line with experience with first desorption of HCP and concrete cured at normal temperatures, the water loss is very gradual, and almost linear in the P/P^o-range covered for HCP50RT. Clearly, both the steam curing and predrying treatment has produced a much coarser pore structure than for HCP50RT, in spite of the lower w/c-ratio.

The adsorption curves for the two steam cured samples are quite different in the low P/P^o-range. The adsorption at $P/P^o = 0.20$ can be taken as a measure of the surface area (or more properly the amount of C-S-H gel produced, i.e. degree of hydration). The ratio is here about 39:27 = 1.4, i.e. indicating 40% more hydration in HCP45ST than in HCP35ST. This appears unreasonable, but we have no other explanation for this result. No value for the chemically bound water is available for either of the ST-cured HCP, but properties for similar pastes have been reported [8, 9, 10] with small differences in chemically bound water.

3.3 Regression Coefficients

The chosen standard form of the isosteric regression equation (Part I, eq. 1) was:

$$\ln P = A + B \cdot \frac{1000}{T} + C \cdot \ln T \qquad (1)$$

For pure water (Table 3) the coefficients were:

A = 47.730; B = -6.4733; C = -4.0105

Tables 5 to 8 give the regression coefficients for the samples HCP35ST, HCP45ST, HCP50RT and PVG, respectively. The P/P^o-values at 20 ºC given in the tables are taken from the regression lines, hence they are appropriate as reference values for plots at other temperatures also based on the regression lines. Moisture contents at each moisture content step are also given in the tables to allow plotting of the sorption isotherms at any desired temperature. The quantity D is the % difference between the heat and cool values of the relative vapor pressure at 20 °C. Table 3 gives the saturated water vapor pressure both from tabulated standard values and as calculated from the A, B and C coefficients given above. As can be seen, the differences are very small.

Figs. 5-8 give sample plots of lnP vs. 1000/T for all the specimens at selected moisture contents to illustrate the results. For HCP35ST, HCP45ST and PVG the heat-cool hysteresis is very small.

For HCP50RT the hysteresis was somewhat greater, unfortunately, however the coefficients for the cool data are not available, but original calculation results for enthalpy and entropy are available, and will be given later. Table 7, column P(4.7 ºC) before and after values give an indication of the hysteresis effect in HCP50RT; as we see "after" values are generally higher, as is expected for desorption steps. The hysteresis is small at high and low moisture contents, and largest in the midrange where capillary effects are prominent. For HCP45ST (only adsorption) the hysteresis was oposite to the expected, with values "after" lower than "before", but the difference is smaller because of the moisture eqilibration procedure at high temperature applied at each step before the slow HEAT/COOL runs, as well as the fact that ST-curing produces a coarser microstructure with improved water mobility.

3.4 Enthalpy and Entropy of adsorption

Equations (2) and (3) are used to calculate the thermodynamic parameters. They are defined in Part I, and repeated here:

$$\Delta h_{st}^{o} = h^{og} - h^{\sigma} = -R \cdot \left(\frac{d \ln P^{g}}{d(1/T)}\right) = -1000 \cdot R \cdot B + R \cdot C \cdot T \qquad (2)$$

and

$$\Delta s_{st}^{o} = s^{og} - s^{\sigma} = R \cdot \left(\frac{d \ln P^{g}}{d \ln T}\right) + R \cdot \ln\left(\frac{P^{g}}{P^{og}}\right) = R \cdot C + R \cdot \ln\left(\frac{P^{g}}{P^{og}}\right) - \frac{1000 \cdot R \cdot B}{T} \qquad (3)$$

Note that the superscript g in the equations indicate gas (i.e. water vapor), this is not general in this report where P is used alone and always meaning vapor pressure. Note also that the enthalpy calculation only involves regression coefficients (B, C), while the entropy equation has an extra term. That is because the entropy of the water vapor is a function of P^{g}/P^{og}, and the extra term is needed to give Δs_{st}^{o} relative to saturated water vapor. The enthalpy is independent of P^{g}/P^{og} when water vapor is considered an ideal gas. σ indicates water in the adsorbed state; to calculate enthalpy and entropy of condensation for bulk water the superscript σ is replaced by l (liquid). The enthalpy and entropy values calculated with eq. (2) and (3) are referred to as isosteric, since they are obtained from P-T data under condition of constant moisture contents. They are also of course differential quantities.

The results of the calculations are shown for enthalpy in Figs. 9 and 10 (vs. Moisture content), and in Fig. 13a-f (vs. P/P^{o}). The entropy data are shown in Figs. 11 and 12 (vs. Moisture content), and in Fig. 14a-e (vs. P/P^{o}). Numerical values for different specimens at selected temperatures are given in Tables 9 to 12. The smoothed lines at 20 °C for all samples are plotted together for enthalpy in Fig. 13b and for entropy in Fig. 14b. The results are discussed below.

The plots of enthalpy and entropy versus moisture contents show large differences between the samples (Figs. 9-12). However, a more systematic picture emerges when the thermodynamic quantities are plottet versus the relative vapor pressure. For each sample the relationship is not always smooth (Figs. 13c – 13f and 14c – 14f), but the collective, smoothed lines for enthalpy (Fig. 13b) and entropy (Fig. 14b) show systematic trends. The enthalpy of adsorption (Fig. 13b) shows increasing values in the order:

Ideal capillary $\rightarrow$ PVG $\rightarrow$ HCP35/45ST $\rightarrow$ HCP50RT

The same is true for the entropy of adsorption (Fig. 14b). As already stated, HCP50RT was tested in the most "virgin" condition during first desorption after long time curing in water at room temperature. It is known that both steam curing and drying/resaturation treatment strongly influence the water sorption behavior (and the pore structure) of HCP. Both lead to a coarsening of the pore structure manifested in that the sorption isotherms are much steeper near saturation (Fig. 4), the water permeability increases and the adsorption at low relative vapor pressures (monolayer and interlayer water capacity) decreases. Calorimetric measurements of ice formation in water saturated HCP also give much higher amounts of ice after such treatment – again demonstrating a more coarse and continous pore structure. These observations are in line with present thermodynamic data showing reduced enthalpy and entropy values with increased fineness of structure. Clearly the solid surface forces play a larger role for RT cured HCP than for ST-curing, and water in HCP generally is more strongly affected than water in PVG.

3.5 Sorption Isotherms at Different Temperatures

This topic is of current practical interest in connection with understanding the variation of the thermal expansion coefficient of concrete with moisture content, Meyers [12] and Bazant [13]. This variation is large, with low values for saturated and dry concrete and significantly higher values in the midrange 50-80% P/P^o. The topic will therefore be explored in some detail using the unique data available here. The basic idea is that when concrete is heated at constant moisture content the resulting expansion is a product of (at least) two major mechanisms in the midrange of P/P^o: The "pure" thermal expansion and the expansion caused by increased P/P^o (or relative humidity, %RH, the more common term). The latter effect may be expressed by the coefficient RH change per degree (%RH/°C).

This %RH change is a result of the basic ln P vs. 1/T plot, f.ex. Fig. 5a. The slopes of the curves is proportional to the enthalpy of adsorption according to eq. (2).

Thus, as the adsorption enthalpy increases, the negative slope of the ln P vs. 1/T increases as Fig. 5a shows. The consequence for RH can be demonstrated as follows using the principle sketch below: We consider heating from T_1 to T_2 (going from right to left in the sketch), with P_1^o and P_2^o as the relevant saturation vapor pressures, and P_1 and P_2 the vapor pressures at some reduced moisture content. Assuming the ln P vs. 1/T lines are straight (merely for convenience), then the negative slopes (eq. (2)) are proportional to the values $(h^{og} - h^l)$ for the water line and $(h^{og} - h^\sigma)$ for the less than saturated line; the latter having the higher numerical value.

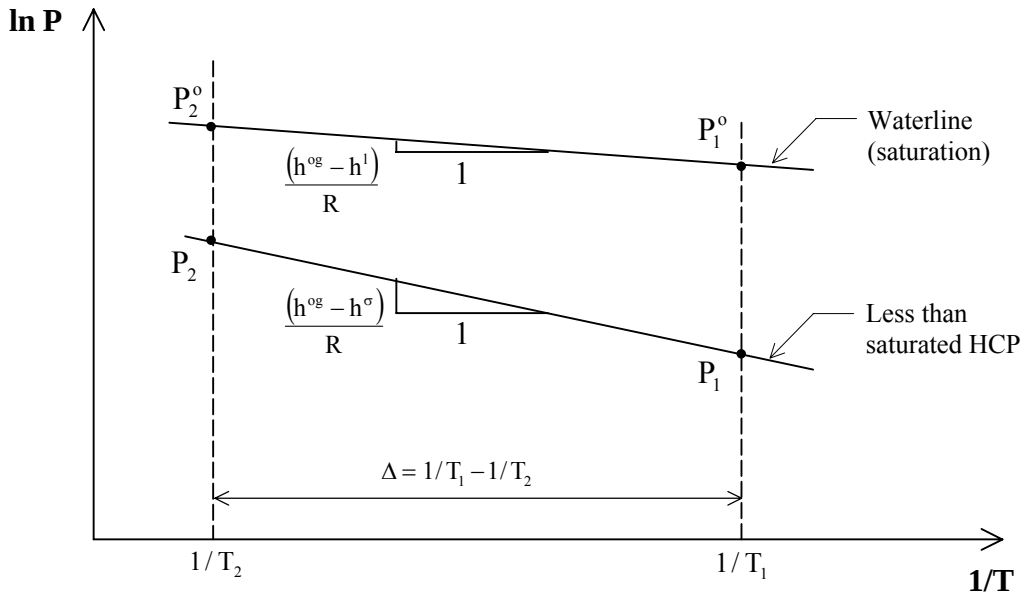

Then: $RH_1 = P_1/P_1^o$ and $RH_2 = P_2/P_2^o$, and:

$\ln P_2 = \ln P_1 + \Delta\cdot(h^{og} - h^\sigma)/R$

$\ln P_2^o = \ln P_1^o + \Delta\cdot(h^{og} - h^l)/R$

Subtracting the second from the first equation yields:

$$\ln \frac{P_2}{P_2^o} = \ln \frac{P_1}{P_1^o} + \Delta \cdot (h^l - h^\sigma)/R$$

and

$$\ln \frac{RH_2}{RH_1} = \Delta \cdot (h^l - h^\sigma)/R$$

and

$$RH_2 = RH_1 \cdot e^{\Delta\cdot(h^l - h^\sigma)/R} \qquad (4)$$

If $h^l = h^\sigma$, i.e.the lines in the sketch are parallel, then $RH_1 = RH_2$ and there is no temperature effect on RH. However, h^l is always greater than h^σ, hence RH always increases with increasing temperature for samples less than saturated. Fig. 13b shows enthalpy values for our four materials and $(h^l - h^\sigma)$ in the plots are the distance between the liquid water line and the curved line for each of the different materials, the difference increasing with decreasing %RH from zero at saturation. The factor %RH/°C can be expressed in terms of enthalpy using eq. (4), and looking at the temperature range 20 °C to 30 °C, when $\Delta = (1/T_1 - 1/T_2) = 1.125\cdot10^{-4}$ and $\Delta T = 10$:

$$\%RH/^oC = \frac{\%RH_2 - \%RH_1}{10} = \frac{\%RH_1}{10} \cdot (e^{\Delta\cdot(h^l - h^\sigma)/R} - 1) \qquad (5)$$

For example, for HCP50RT at $RH_1 = 71.6\%$ at 20 °C and moisture content = 229.8 g/g_{dry} (Table 7) the enthalpy of adsorption $(h^{og} - h^\sigma)$ is 11.40 kcal/mole (Table 9), while for pure water $(h^{og} - h^l)$ is 10.56 kcal/mole (Table 2). According to eq. (5) with R = 1.99 cal/K·mole, this gives

%RH/°C = 0.34. The same calculation gives 0.27 %RH/°C at RH_1 = 26.7% at 20 °C. Thus, in spite of the fact that (h^l - h^σ) always increases with decreasing RH_1 (Fig. 13) the %RH/°C vs. RH goes through a maximum at intermediate RH-values since it is zero at saturation. The reason is that the term in brackets in eq. (5) always increases with decreasing RH, but it is multiplied by RH_1 which of course decreases, and the factor %RH/°C is again zero in the dry state (RH_1 = 0).

We shall also examine the RH-T effect for the case of pure water in capillary tension. The Kelvin-laPlace equation:

$$\ln \frac{p}{p^o}(T) = \frac{2}{r_k \cdot R} \cdot \frac{\sigma(T)}{T} \qquad (6)$$

relates the meniscus radius (r_k), the surface tension of the water-vapor interface ($\sigma(T)$), the gas constant (R) and the absolute temperature (T) to the vapor pressure exerted by the water under capillary tension. $\sigma(T)$ varies with temperature as follows: 0 ºC (76.0 dynes/cm), 10 ºC (74.5), 20 ºC (73.0), 30 ºC (71.4), 40 ºC (70.0). Assuming that a constant moisture content in a sample implies a constant r_k, i.e. ignoring the second order effects of thermal expansion as well as any internal redistribution of moisture in the HCP because of the temperature change. We can then calculate the RH change caused by temperature for different initial RH-values at 20 ºC. This calculation is carried out and the results plotted in Fig. 15a and b for heat and cool, respectively. Only Fig. 15a (heat) is discussed in the following since the most relevant specimen (HCP50RT) only has heat data. Note that the calculation is only carried out in the range 50 – 100 %RH. Capillary water cannot exist below about RH = 45 %RH, since capillary theory is not applicable in this range because the implied tension (about 100 MPa) exceeds the capacity of water, and, in any case, the implied meniscus radius is only the equivalent of about 4 water molecules – much too small a system to apply a "bulk" theory such as the Kelvin-laPlace equation.

Fig. 15a also shows the results for the tested specimens. For HCP50RT the %RH/ºC is calculated as the average in the 15 – 25 ºC range, for the others in the 10 – 30 ºC range. The calculations are made at each ADS/DES-step using the regression coefficients given in Tables 5-8. The figure gives noteworthy information:

Fig. 15a does not show smooth variation for all specimens, but demonstrates a clear overall tendency. The factor %RH/°C increases strongly as RH reduces from saturation, and goes through maximum in the RH-midrange, before reducing on further drying. PVG is closest to the ideal capillary curve, as expected from eq. 5 and the enthalpy data in Fig. 13b. HCP50RT is at the other extreme, as expected, and the ideal capillary effect can only explain part of the RH-change with temperature. It seems that even quite close to saturation the combined effects of very high surface area (strong effects of surface forces) and dissolved ions in the pore water produces effects in excess of the tension associated with capillary condensed water. The two steam cured samples fall between the two extremes, as was also the case for enthalpy in Fig. 13b.

Fig. 15c shows the %RH/°C-factor from from Nilsson [14] and Persson [15] together with the trend line for HCP50RT. Considering the sensivity of such measurements ([14] and [15] are based on measured sorption isotherms at different temperatures) there is a general agreement between the data sets. The implication with respects to variations in the coefficient of thermal expansion (CTE) is as follows [16]: A cement paste with w/c = 0.40 (corresponding to the binder in a high performance concrete) may self desiccate to RH = 88% in a few days. In this state the CTE may be about $22 \cdot 10^{-6}$ per °C, compared to a value of about $11 \cdot 10^{-6}$ per °C at saturation [16]. According to Fig. 15c RH = 88% corresponds to a factor of about 0.15 %RH/°C. Isothermal

shrinkage for such a paste is around $60 \cdot 10^{-6}$ per %RH [16]. Consequently the RH increase of 0.15% will produce an expansion of $0.15 \cdot 60 \cdot 10^{-6} = 9 \cdot 10^{-6}$ per °C, and thereby account for most of the increase in CTE because of self desiccation. Thus, keeping the paste saturated during curing will reduce the CTE significantly and thereby reduce the risk of cracking during the normal cooling phase of concrete elements which follows the initial heating caused by hydration. In structural concrete inclusion of an internal water source such as wet light weight aggregate particles is a practical way to achieve this effect.

Sorption isotherms for the specimens are shown at selected temperatures in Figs. 16 to 19. The selected temperatures differ since the experimental T-ranges were quite different (Table 4), and the uncertainty of the data increases when they are extrapolated outside the measured range.

4. CONCLUSION

The TPA-system has been used to generate water vapor pressure – temperature data for room temperature – and steam cured hardened cement pastes as well as porous vycor glass. The moisture contents range from saturated to dry and the temperatures range from 2 to 95 °C, differing for the specimen types. The data has been analyzed to yield differential enthalpy and entropy of adsorption, as well as the dependence of the relative vapor pressure on temperature at various constant moisture contents. The implications for the coefficient of thermal expansion have been explored.

The main conclusions are:

Both enthalpy and entropy of adsorbed water in hardened cement paste and porous vycor glass decrease strongly with the relative vapor pressure exerted by the pore water. At saturation the values correspond to bulk water, reducing to values lower than for ice (extrapolated to 20 °C) in the relative vapor pressure range below about 30% for hardened cement paste cured at room temperature and about 10% for porous vycor glass.

Both enthalpy and entropy of adsorbed water decreases at any relative vapor pressure in the order:

Porous vycor glass
↓
Steam cured hardened cement paste
↓
Room temperature cured hardened cement paste

This implies fines pore structure and increasing influence of solid surface forces in the same order.

For a sample with fixed moisture content in equilibrium with a water vapor pressure less than saturation, a temperature increase results in an increase in the relative vapor pressure (relative humidity). This implies that the thermal expansion coefficient increases as the moisture content is reduced from saturation, since the relative humidity increase on heating produces swelling in addition to the pure thermal effect. The effect is quantified.

5. REFERENCES

PART I

1. Powers, T.C.; Brownyard, T.L.: Studies of the Physical Properties of Hardened Portland Cement Paste. Research Laboratories of the Portland Cement Association, PCA Bulletin 22, 1948.
2. Hansen, T.C.; Radjy, F.; Sellevold, E.J.: Cement Paste and Concrete. Annual Review of Materials Science, Vol. 3, 1973, pp. 233-268.
3. Second Proposal and Application to the Danish Science Fund (STVF) (ca. 1971)
4. MKS Instruments Inc., Tech. Data Bull. 90, 10-1-1966.
5. MKS Instruments Inc., Tech. Data Bull. 77, 2-9-1966.
6. Bain, R.W.: Steam Tables. Dept. of Scientific and Industrial Research, National Engineering Laboratory, Edinburgh. Her Majesty's Stationery Office, 1964.
7. Adamson, W.A.: Physical Chemistry of Surfaces. Interscience, New York, 1960.

PART II

8. Radjy, F.; Richards, C.W.: Materials and Structures 2, 1969.
9. Bray, W.H.; Sellevold, E.J.: Water Sorption Properties of Hardened Cement Paste Cured or Stored at Elevated Temperatures. Cement and Concrete Research, Vol. 3, 1973, pp. 723-728.
10. Sellevold, E.J.: Mercury Porosimetry of Hardened Cement Paste Cured or Stored at 97 ºC. Cement and Concrete Research, Vol. 4, 1974, pp. 399-404.
11. Sellevold, E.J.; Radjy, F.: Low temperature dynamic mechanical response of porous Vycor glass as a function of moisture content. Part 1 The capillary transition. Journal of Materials Science 11, 1976, pp. 1927-1938.
12. Meyers, S.L.: How Temperature and Moisture Changes May Affect the Durability of Concrete. Rock Products, August 1951, pp. 153-178.
13. Bazant, Z.P.: Delayed Thermal Dilatations of Cement Paste and Concrete due to Mass Transport. Nuclear Eng. And Design, 1970, pp. 308-318.
14. Nilsson, L-O.: Temperature Effekts in Relative Humidity Measurements on Concrete – Some Preliminary Studies, The Moisture Group, Report 1987:1. BFR, 84, 1987.
15. Persson, Bertil: Self-desiccation and chloride migration. Report TVBM-3104, Lund University, Division of Building Materials, Sweden, June 2002, pp. 175-194.
16. Sellevold, E.J.; Bjøntegaard, O.: Coefficient of Thermal Expansion in Concrete: Effects of Moisture. Report TVBM-3104, Lund University, Division of Building Materials, Sweden, June 2002, pp. 67-75.
17. Olesen, R.; Hansen, K.K.: "Dokumentation til programsystemet ISOTERM". Teknisk Rapport 248/91, Laboratoriet for bygningsmaterialer, Danmarks Tekniske Universitet, 1991 (in Danish).
18. Hansen, M.H.: Estimation of transfer coefficients in models for coupled heat and moisture transfer in porous media. PhD thesis. Technical Report 283/93. Building Materials Laboratory, Technical University of Denmark, 1993, pp. 16-23.

Table 5 Regression Coefficients HCP35ST

ADS/ DES	u $\left[\frac{mg}{g_{dry}}\right]$	HEAT				COOL				D
		P/P^o 20°C	A	B	C	P/P^o 20°C	A	B	C	
DRY	0	0.000	-79.8941	-3.28748	15.1974	0.000	47.73	-6.4733	-4.0105	-1.31
ADS	5.2	0.001	118.636	-13.0024	-13.8036	0.001	-25.0124	-5.8699	7.08932	-25.80
ADS	11.4	0.009	102.93	-11.1743	-11.7247	0.009	27.5912	-8.28627	-0.568122	4.89
ADS	16.5	0.038	106.488	-10.709	-12.3847	0.035	95.8937	-10.8479	-10.6909	8.37
ADS	21.8	0.098	88.5233	-9.4118	-9.8354	0.092	111.438	-11.0022	-13.0954	6.24
ADS	26.7	0.186	106.577	-9.99073	-12.5534	0.173	91.0871	-9.57295	-10.2013	6.75
ADS	31.4	0.278	103.713	-9.68769	-12.1604	0.264	102.607	-9.87007	-11.9393	4.93
ADS	36.3	0.370	77.3228	-8.29926	-8.29806	0.342	78.4007	-8.49682	-8.42856	7.61
ADS	41.5	0.446	77.9778	-8.265227	-8.40116	0.439	105.723	-9.73097	-12.4517	1.61
ADS	46.6	0.516	66.6894	-7.68716	-6.73532	0.501	63.486	-7.57576	-6.26697	2.95
ADS	51.5	0.578	74.3894	-7.98749	-7.8906	0.568	61.8909	-7.47937	-6.02067	1.71
ADS	64.6	0.720	63.4655	-7.34585	-6.31419	0.734	66.8925	-7.65167	-6.77558	-1.99
ADS	72.2	0.802	56.2007	-6.96346	-5.24602	0.799	53.3036	-6.89197	-4.79443	0.39
ADS	80.1	0.861	46.6406	-6.51618	-3.81902	0.860	70.4393	-7.65388	-7.33861	0.14
ADS	91	0.919	57.4675	-6.97298	-5.43929	0.841	52.306	-6.77627	-4.66039	8.46
ADS	103.5	0.964	57.6023	-6.98083	-5.44978	0.966	136.023	-10.7868	-16.9932	-0.20
ADS	117.3	0.982	60.5209	-7.09092	-5.89435	0.975	63.3017	-7.2225	-6.30761	0.67
ADS	135.3	0.984	57.803	-6.97289	-5.48632	0.988	65.4371	-7.32575	-6.61994	-0.37
ADS	153.5	1.001	67.2654	-7.39534	-6.8954	0.999	52.1822	-6.68879	-4.66682	0.21
ADS	179.7	0.997	52.3181	-6.6956	-4.68504	0.997	77.019	-7.8287	-8.35251	0.00
DES	155.1	0.965	42.429	-6.26505	-3.20854	0.976	52.3386	-6.69649	-4.68812	-1.21
DES	120.9	0.936	36.2127	-5.97232	-2.29524	0.944	55.1173	-6.801	-5.11817	-0.79
DES	86.8	0.733	78.0303	-8.07577	-8.43655	0.728	53.5326	-6.76155	-4.86883	0.70
DES	66.6	0.527	73.4427	-8.11807	-7.66182	0.581	54.3071	-6.99485	-4.91075	-10.31
DES	50.6	0.339	89.3172	-8.97783	-10.0176	0.353	88.5772	-8.70911	-9.95384	-4.14
DES	44.7	0.258	90.9501	-9.24855	-10.1905	0.291	93.3762	-9.14682	-10.6235	-12.72
DES	36.8	0.084	89.2516	-9.70035	-9.81677	0.092	99.8877	-9.54722	-11.5634	-8.72
DES	29	0.026	75.3356	-9.49611	-7.69603	0.029	104.713	-10.3275	-12.1472	-12.24
DES	24.1	0.012	104.41	-11.2904	-11.8741	0.015	130.506	-12.0329	-15.8643	-21.14
DES	9	0.001	-313.205	8.91479	49.0942	0.001	88.0186	-10.29	-9.55562	39.19

$$D = 100 \cdot \frac{\left(\frac{P}{P^o}\right)_{HEAT} - \left(\frac{P}{P^o}\right)_{COOL}}{\left(\frac{P}{P^o}\right)_{HEAT}}$$

Table 6 Regression Coefficients HCP45ST

ADS/ DES	u $\left[\frac{mg}{g_{dry}}\right]$	HEAT				COOL				D
		P/P^o 20°C	A	B	C	P/P^o 20°C	A	B	C	
ADS	14.8	0.002	262.21	-19.481	-35.014	0.004	79.042	-10.188	-8.2784	-50.53
ADS	25	0.027	140.28	-12.512	-17.309	0.024	181.8	-14.598	-23.386	11.07
ADS	30.2	0.061	91.695	-9.8649	-10.206	0.062	105.25	-10.497	-12.208	-2.64
ADS	36.2	0.134	96.906	-9.7592	-11.047	0.137	72.591	-8.591	-7.465	-1.84
ADS	42.2	0.236	95.982	-9.4106	-10.995	0.226	88.554	-9.1178	-9.8703	3.93
ADS	48.2	0.334	81.423	-8.5879	-8.8645	0.330	81.982	-8.6477	-8.9295	1.41
ADS	54.1	0.440	95.44	-9.1204	-10.964	0.426	93.999	-9.105	-10.725	3.03
ADS	60.1	0.510	69.254	-7.8384	-7.0981	0.512	51.562	-7.0286	-4.4691	-0.49
ADS	66	0.598	66.345	-7.635	-6.6802	0.580	85.268	-8.5608	-9.4606	2.92
ADS	72	0.671	67.303	-7.6406	-6.8251	0.667	52.064	-6.9352	-4.5671	0.57
ADS	78.6	0.740	75.188	-7.9285	-8.023	0.716	89.868	-8.6831	-10.16	3.32
ADS	84.6	0.801	89.284	-8.5253	-10.132	0.786	73.133	-7.855	-7.6948	1.93
ADS	92	0.857	43.735	-6.4078	-3.3736	0.840	80.056	-8.1327	-8.735	1.93
ADS	100	0.904	61.063	-7.1552	-5.9657	0.887	97.944	-8.9145	-11.405	1.91
ADS	110.4	0.946	73.455	-7.7218	-7.7989	0.941	56.455	-6.953	-5.2689	0.53
ADS	122.3	0.972	76.769	-7.8117	-8.3234	0.949	84.883	-8.2559	-9.4893	2.41
ADS	136.23	0.979	53.676	-6.7697	-4.8827	4.107	1074.7	-53.292	-156.43	-319.41

$$D = 100 \cdot \frac{\left(\frac{P}{P^o}\right)_{HEAT} - \left(\frac{P}{P^o}\right)_{COOL}}{\left(\frac{P}{P^o}\right)_{HEAT}}$$

Table 7 Regression Coefficients HCP50RT

P(4.7 °C)* [Torr] Before	After	ADS/ DES	u $\left[\frac{mg}{g_{dry}}\right]$	HEAT			
				P/P^o 20°C	A	B	C
6.19	6.18	DES	320.3	1.005	179.609	-12.323	-23.712
6.03	6.01	DES	306.7	0.978	246.223	-15.101	-33.775
5.58	5.64	DES	286.8	0.915	157.569	-11.38	-20.415
5.15	5.19	DES	267	0.867	91.752	-8.588	-10.515
4.63	4.71	DES	248.5	0.788	58.741	-7.267	-5.514
4.22	4.34	DES	229.8	0.714	-2.975	-4.641	3.756
3.92	4.02	DES	211.8	0.652	109.084	-9.581	-13.02
3.24	3.41	DES	192.4	0.565	-36.31	-3.292	8.773
3.38	3.45	DES	178.9	0.592	20.971	-5.794	0.2
2.61	2.83	DES	166	0.460	-56.13	-2.64	11.834
2.32	2.47	DES	139.1	0.414	26.469	-6.153	-0.615
1.88	2.10	DES	126.6	0.345	-98.455	-0.706	18.073
1.36	1.52	DES	112.9	0.254	-74.6	-2.014	14.605
1.46	1.50	DES	103.9	0.271	97.706	-9.519	-11.209
1.42	1.44	DES	98	0.266	115.468	-10.241	-13.905

* The vapor pressure was read manually by balancing the measuring bridge before and after a HEAT/COOL run.

Table 8 Regression Coefficients PVG

ADS/ DES	u $\left[\frac{mg}{g_{dry}}\right]$	HEAT				COOL				D
		P/P^o 20°C	A	B	C	P/P^o 20°C	A	B	C	
DRY	0	0.001	-56.4956	-3.71046	11.437	0.001	153.457	-14.2152	-19.2739	28.85
ADS	5.9	0.015	107.942	-10.8459	-12.728	0.014	96.1484	-10.3077	-10.9811	3.35
ADS	9.9	0.037	61.2522	-8.26249	-5.89598	0.036	27.0224	-6.64707	-0.843674	1.85
ADS	15.1	0.083	76.3543	-8.72331	-8.13669	0.079	76.1543	-8.77069	-8.08149	4.69
ADS	20.4	0.145	77.7353	-8.60167	-8.35436	0.140	75.7155	-8.53361	-8.04502	2.99
ADS	25.7	0.225	78.0151	-8.44095	-8.42227	0.222	72.5991	-8.19627	-7.61817	1.34
ADS	40.6	0.463	43.7219	-6.56379	-3.38581	0.458	58.1119	-7.24685	-5.51091	1.20
ADS	61.3	0.620	60.876	-7.28818	-5.91931	0.617	44.7282	-6.51905	-3.53943	0.48
ADS	91.4	0.721	47.2893	-6.59747	-3.9158	0.714	47.1597	-6.58947	-3.89951	0.97
ADS	154	0.762	64.1331	-7.3638	-6.41093	0.769	33.6647	-5.92161	-1.91192	-0.87
ADS	194.2	0.789	66.6105	-7.47206	-6.77598	0.777	38.4816	-6.18636	-2.59894	1.45
ADS	213.8	0.818								
ADS	223.9	0.989	9.27509	-4.67965	1.68007	0.977	53.4849	-6.74845	-4.8623	1.24
ADS	227.8	0.997	51.6645	-6.6647	-4.5885	0.997	52.1329	-6.68614	-4.65809	0.01
DES	223.9	0.994	64.1509	-7.24974	-6.43575	0.998	44.271	-6.30899	-3.50035	-0.43
DES	222.2	0.993	38.9674	-6.08915	-2.69975					
DES	217.1	0.810	35.2234	-6.14925	-2.04035	0.798	-3.02626	-4.42418	3.65448	1.44
DES	213.1	0.758	67.693	-7.66496	-6.85769					
DES	157.4	0.705	58.9973	-7.18398	-5.62859	0.688	83.0402	-8.32883	-9.17776	2.39
DES	90.8	0.676	61.951	-7.29497	-6.08921	0.710	77.9416	-7.95556	-8.49888	-4.98
DES	57.9	0.578	48.4972	-6.71637	-4.09578	0.576	50.5019	-6.81599	-4.38959	0.42
DES	38.9	0.380	54.4024	-7.16396	-4.94033	0.385	60.5381	-7.42931	-5.85879	-1.31
DES	29.2	0.215	66.8421	-7.97848	-6.7412	0.225	80.8399	-8.60119	-8.82354	-4.55

$$D = 100 \cdot \frac{\left(\frac{P}{P^o}\right)_{HEAT} - \left(\frac{P}{P^o}\right)_{COOL}}{\left(\frac{P}{P^o}\right)_{HEAT}}$$

Table 9. HEAT-COOL effects for HCP50RT. Entropy and Enthalpy at 20 ºC.

Moisture content [mg/g_{dry}]	**Enthalpy** [kcal/mole]		**Entropy** [cal/mole/ºC]	
	HEAT	COOL	HEAT	COOL
Water	10.56		36.02	
320.3	10.78	11.15	36.40	37.98
306.7	10.37	10.67	35.18	36.36
286.8	10.76	10.93	36.38	37.11
267.0	10.93	11.04	37.01	37.38
248.5	11.22	11.14	37.41	37.58
229.8	11.40	11.32	38.24	37.99
211.8	11.45	11.20	38.30	37.48
192.4	11.65	-	38.60	-
178.9	11.62	11.36	38.60	37.76
166.0	12.13	11.72	39.85	38.58
139.1	11.89	11.58	38.79	37.87
126.6	11.92	11.82	38.56	38.35
112.9	12.50	12.17	39.93	39.00
103.9	12.38	12.19	39.63	39.03
98.0	12.24	11.98	39.14	38.26

Table 10 Enthalpy and Entropy, HEAT and COOL, HCP35ST, ADS/DES, 20 ºC, 50 ºC

ADS/ DES	u $\left[\frac{mg}{g_{dry}}\right]$	20°C				50°C			
		H [kcal/mole]		S [cal/(mole·K)]		H [kcal/mole]		S [cal/(mole·K)]	
		HEAT	COOL	HEAT	COOL	HEAT	COOL	HEAT	COOL
DRY	0.0	15.39	15.79	37.30	38.72	16.29	16.22	38.16	36.78
ADS	5.2	17.80	16.14	46.80	41.59	16.97	16.10	42.05	38.17
ADS	11.4	15.38	15.33	43.19	42.93	14.68	14.69	38.84	37.56
ADS	16.5	14.07	14.23	41.50	41.90	13.33	13.45	37.02	36.06
ADS	21.8	12.97	13.08	39.64	39.88	12.39	12.47	35.66	34.60
ADS	26.7	12.54	12.66	39.44	39.70	11.79	11.95	34.93	34.08
ADS	31.4	12.17	11.97	38.96	38.20	11.44	11.47	34.53	33.27
ADS	36.3	11.66	12.08	37.79	39.09	11.16	11.34	34.11	33.37
ADS	41.5	11.53	11.40	37.73	37.26	11.03	11.03	34.02	32.74
ADS	46.6	11.35	11.36	37.41	37.36	10.95	11.00	34.03	32.89
ADS	51.5	11.28	11.26	37.38	37.28	10.81	10.85	33.77	32.66
ADS	64.6	10.92	10.90	36.60	36.58	10.54	10.62	33.30	32.34
ADS	72.2	10.78	10.93	36.34	36.85	10.47	10.50	33.25	32.13
ADS	80.1	10.72	10.75	36.29	36.37	10.50	10.47	33.47	32.17
ADS	91.0	10.69	11.54	36.29	39.01	10.36	10.52	33.16	32.41
ADS	103.5	10.70	10.68	36.42	36.36	10.37	10.30	33.29	31.83
ADS	117.3	10.66	10.70	36.32	36.45	10.31	10.31	33.10	31.87
ADS	135.3	10.66	10.57	36.33	36.04	10.33	10.30	33.19	31.83
ADS	153.5	10.68	10.69	36.43	36.47	10.27	10.19	33.02	31.55
ADS	179.7	10.58	10.58	36.07	36.07	10.30	10.30	33.09	31.86
DES	155.1	10.58	10.53	36.02	35.88	10.39	10.23	33.32	31.59
DES	120.9	10.53	10.60	35.79	36.05	10.39	10.31	33.27	31.80
DES	86.8	11.13	11.04	37.36	37.03	10.63	10.75	33.65	32.77
DES	66.6	11.67	11.51	38.53	38.18	11.21	10.91	34.97	32.94
DES	50.6	12.01	11.99	38.80	38.82	11.41	11.35	34.79	33.46
DES	44.7	12.44	12.24	39.75	39.29	11.83	11.55	35.70	33.74
DES	36.8	13.56	13.45	41.34	41.12	12.97	12.72	37.36	35.47
DES	29.0	14.39	14.67	41.84	43.03	13.93	13.72	38.27	36.65
DES	24.1	15.52	14.88	44.15	42.35	14.81	14.31	39.77	37.20
DES	9.0	10.88	14.34	23.67	34.48	13.81	15.36	31.10	34.47

Table 11 Enthalpy and Entropy, HEAT and COOL, HCP45ST, 20 ºC, 50 ºC

ADS/ DES	**u** $\left[\frac{mg}{g_{dry}}\right]$	**20°C**				**50°C**			
		H [kcal/mole]		S [cal/(mole·K)]		H [kcal/mole]		S [cal/(mole·K)]	
		HEAT	COOL	HEAT	COOL	HEAT	COOL	HEAT	COOL
ADS	14.8	18.32	15.42	-21.01	41.47	16.29	16.22	38.16	36.78
ADS	25	14.78	15.39	43.28	45.11	16.97	16.10	42.05	38.17
ADS	30.2	13.66	13.75	41.03	41.38	14.68	14.69	38.84	37.56
ADS	36.2	12.96	12.72	40.22	39.45	13.33	13.45	37.02	36.06
ADS	42.2	12.30	12.37	39.07	39.24	12.39	12.47	35.66	34.60
ADS	48.2	11.90	11.98	38.42	38.67	11.79	11.95	34.93	34.08
ADS	54.1	11.74	11.85	38.40	38.71	11.44	11.47	34.53	33.27
ADS	60.1	11.44	11.36	37.69	37.44	11.16	11.34	34.11	33.37
ADS	66	11.28	11.50	37.46	38.15	11.03	11.03	34.02	32.74
ADS	72	11.21	11.12	37.44	37.13	10.95	11.00	34.03	32.89
ADS	78.6	11.08	11.34	37.20	38.01	10.81	10.85	33.77	32.66
ADS	84.6	11.04	11.13	37.22	37.48	10.54	10.62	33.30	32.34
ADS	92	10.77	11.07	36.43	37.43	10.47	10.50	33.25	32.13
ADS	100	10.74	11.07	36.45	37.53	10.50	10.47	33.47	32.17
ADS	110.4	10.80	10.75	36.74	36.54	10.36	10.52	33.16	32.41
ADS	122.3	10.67	10.88	36.36	37.00	10.37	10.30	33.29	31.83
ADS	136.23	10.61	14.77	36.15	53.20	10.31	10.31	33.10	31.87

Table 12 Enthalpy and Entropy, HEAT and COOL, PVG, ADS/DES, 20 ºC, 50 ºC

ADS/ DES	**u** $\left[\frac{mg}{g_{dry}}\right]$	**20°C**				**50°C**			
		H [kcal/mole]		S [cal/(mole·K)]		H [kcal/mole]		S [cal/(mole·K)]	
		HEAT	COOL	HEAT	COOL	HEAT	COOL	HEAT	COOL
DRY	0	14.04	17.02	33.87	43.38	14.72	15.87	32.78	36.34
ADS	5.9	14.14	14.09	39.83	39.59	13.38	13.43	34.06	34.15
ADS	9.9	12.98	12.72	37.75	36.80	12.63	12.67	33.30	33.33
ADS	15.1	12.59	12.72	38.01	38.35	12.11	12.24	33.13	33.48
ADS	20.4	12.23	12.27	37.87	37.96	11.73	11.79	32.94	33.10
ADS	25.7	11.87	11.85	37.52	37.43	11.37	11.40	32.59	32.65
ADS	40.6	11.07	11.19	36.24	36.62	10.87	10.86	32.28	32.25
ADS	61.3	11.03	10.89	36.69	36.20	10.68	10.68	32.24	32.21
ADS	91.4	10.83	10.82	36.29	36.25	10.60	10.59	32.23	32.19
ADS	154	10.90	10.65	36.64	35.82	10.52	10.54	32.09	32.14
ADS	194.2	10.90	10.78	36.71	36.27	10.50	10.62	32.10	32.46
ADS	223.9	10.28	10.58	35.04	36.04	10.38	10.29	32.06	31.79
ADS	227.8	10.57	10.57	36.05	36.06	10.30	10.30	31.86	31.85
DES	223.9	10.66	10.50	36.34	35.81	10.27	10.29	31.79	31.82
DES	222.2	10.53	0.00	35.90		10.37		32.07	
DES	217.1	11.03	10.92	37.21	36.81	10.91	11.14	33.51	33.88
DES	213.1	11.24	0.00	37.78		10.83		33.15	
DES	194.9	11.00	11.20	45.44	36.80	10.66	10.66	32.42	32.02
DES	157.4	10.95	10.86	36.82	37.48	10.59	10.35	32.09	30.37
DES	90.8	10.96	10.99	36.57	36.36	10.72	10.73	32.20	30.63
DES	57.9	11.36	11.35	36.30	36.38	11.06	11.00	32.56	
DES	38.9	11.93	11.95	36.82	36.82	11.53	11.43	33.03	
DES	29.2	14.04	17.02	37.64	37.81	14.72	15.87	32.78	36.34

Fig. 3. Zero (dry) isosteres calculated from regression analysis of the experimental data.

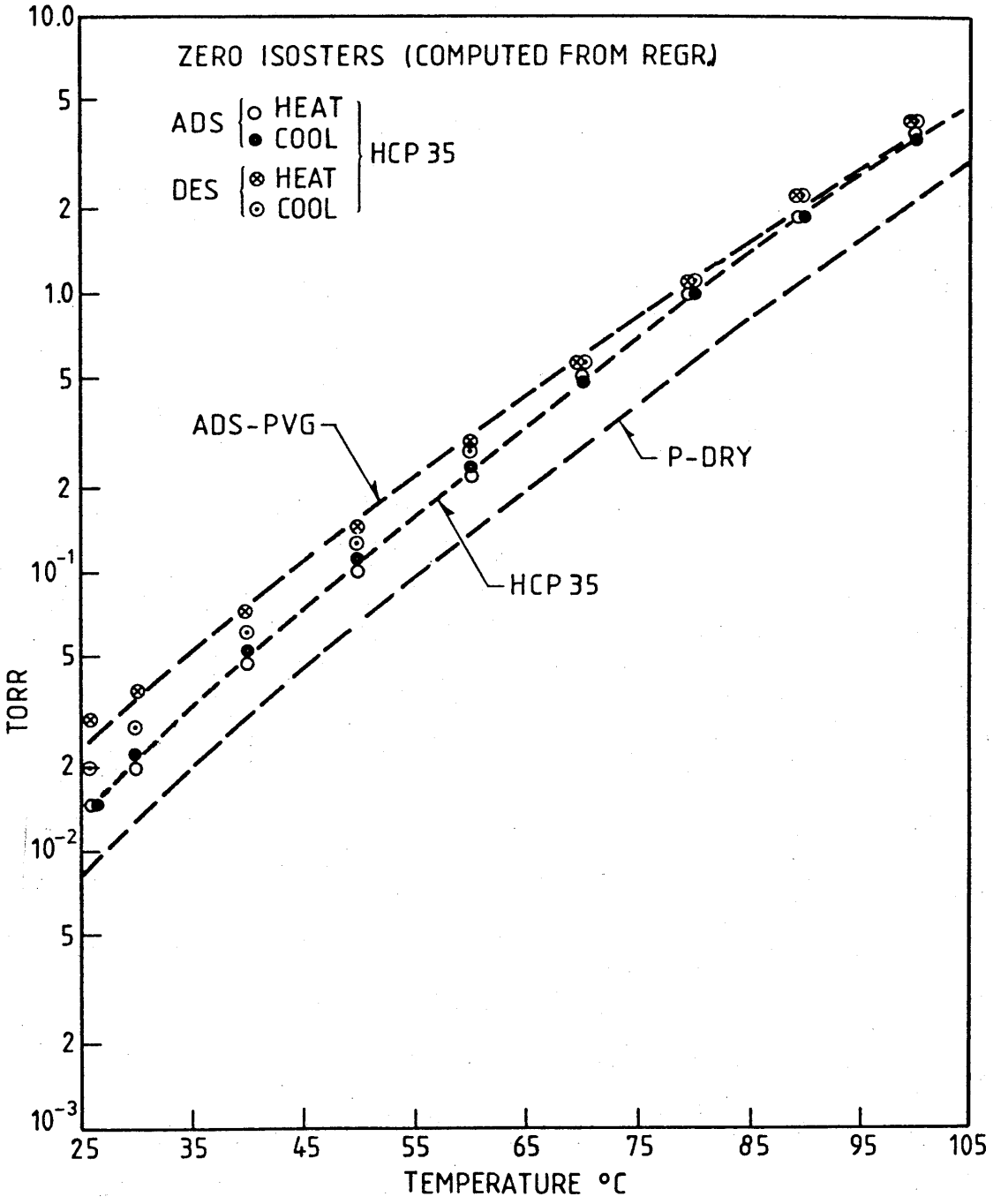

Fig. 4a.

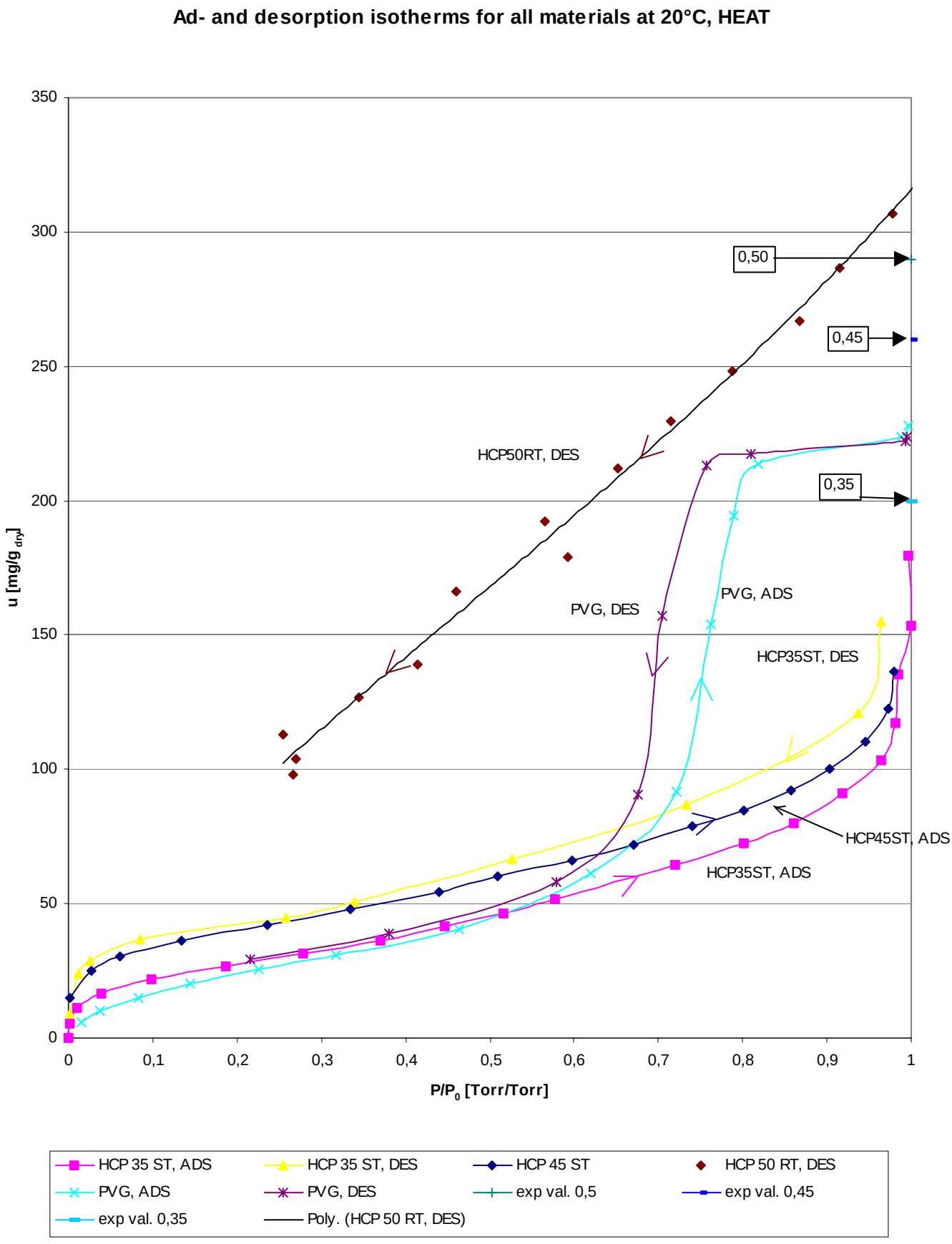
Ad- and desorption isotherms for all materials at 20°C, HEAT
u [mg/g dry]
P/P0 [Torr/Torr]
0,50
0,45
0,35
HCP50RT, DES
PVG, DES
PVG, ADS
HCP35ST, DES
HCP45ST, ADS
HCP35ST, ADS
HCP 35 ST, ADS
HCP 35 ST, DES
HCP 45 ST
HCP 50 RT, DES
PVG, ADS
PVG, DES
exp val. 0,5
exp val. 0,45
exp val. 0,35
Poly. (HCP 50 RT, DES)

Fig. 4b. Sorption Isotherms, HCP35ST (ADS/DES) and HCP45ST (ADS)

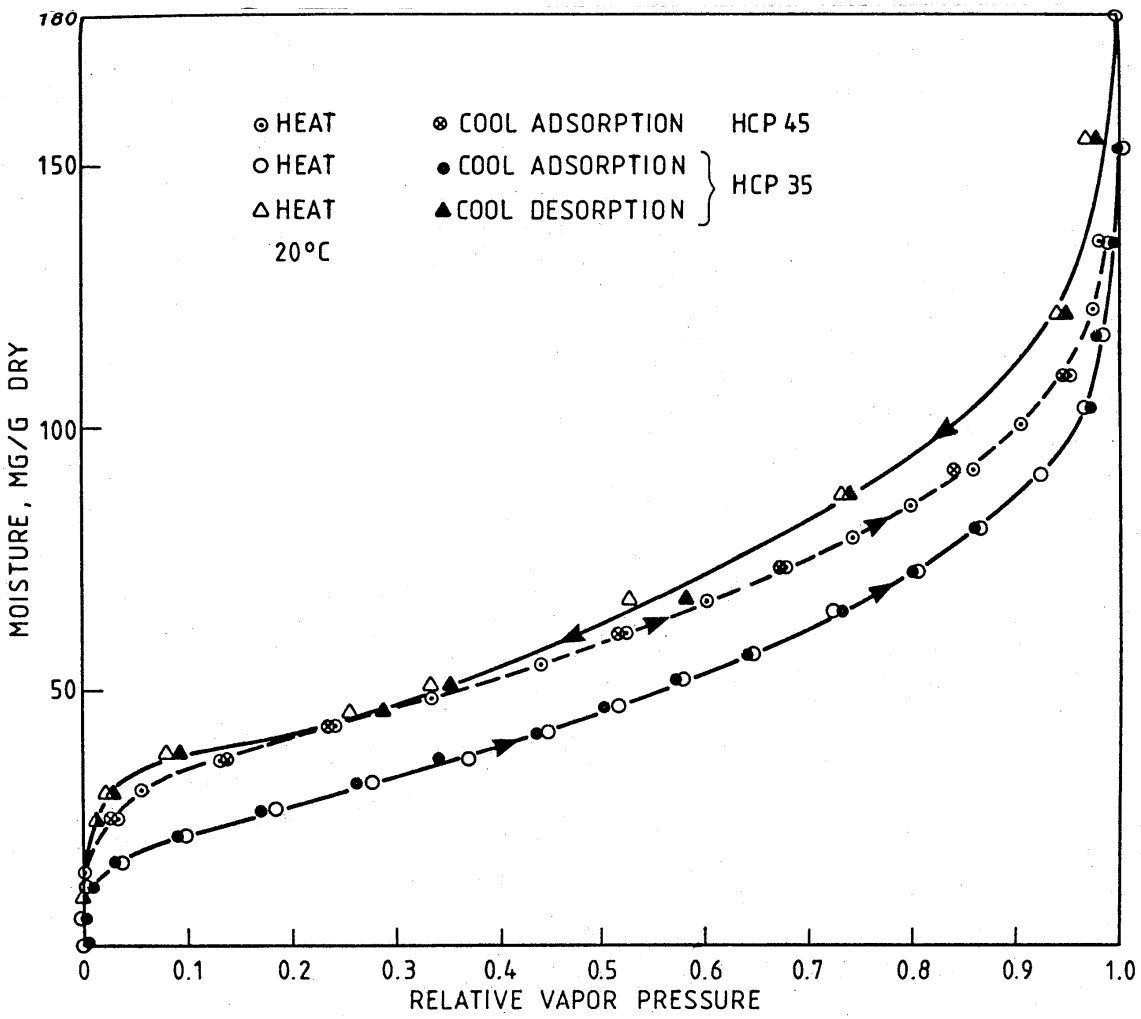

Fig. 5a-c.

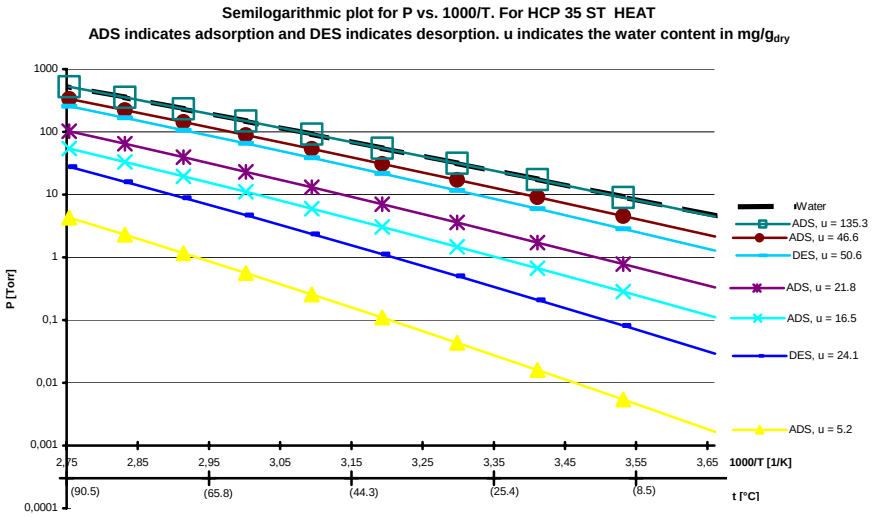
Semilogarithmic plot for P vs. 1000/T. For HCP 35 ST HEAT
ADS indicates adsorption and DES indicates desorption. u indicates the water content in mg/g$_{dry}$
P [Torr]
1000
100
10
1
0,1
0,01
0,001
0,0001
2,75
2,85
2,95
3,05
3,15
3,25
3,35
3,45
3,55
3,65
1000/T [1/K]
(90.5)
(65.8)
(44.3)
(25.4)
(8.5)
t [°C]
Water
ADS, u = 135.3
ADS, u = 46.6
DES, u = 50.6
ADS, u = 21.8
ADS, u = 16.5
DES, u = 24.1
ADS, u = 5.2

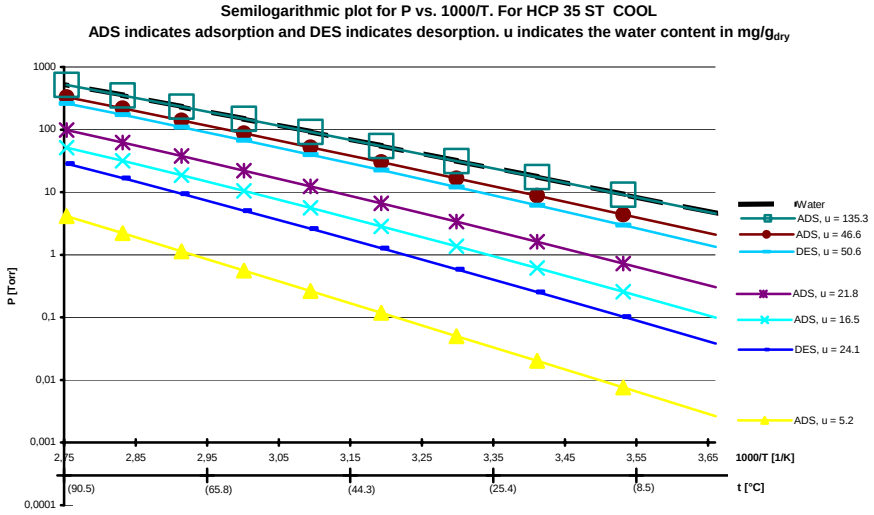
Semilogarithmic plot for P vs. 1000/T. For HCP 35 ST COOL
ADS indicates adsorption and DES indicates desorption. u indicates the water content in mg/g$_{dry}$
P [Torr]
1000
100
10
1
0,1
0,01
0,001
0,0001
2,75
2,85
2,95
3,05
3,15
3,25
3,35
3,45
3,55
3,65
1000/T [1/K]
(90.5)
(65.8)
(44.3)
(25.4)
(8.5)
t [°C]
Water
ADS, u = 135.3
ADS, u = 46.6
DES, u = 50.6
ADS, u = 21.8
ADS, u = 16.5
DES, u = 24.1
ADS, u = 5.2

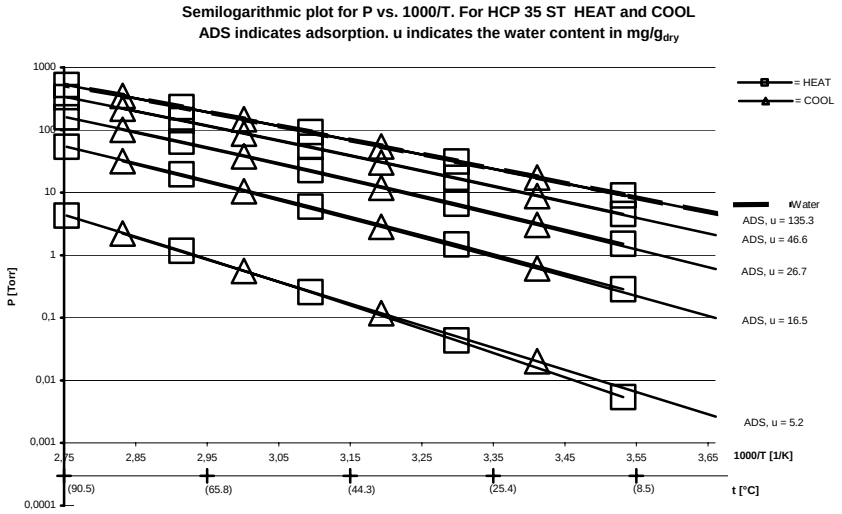
Semilogarithmic plot for P vs. 1000/T. For HCP 35 ST HEAT and COOL
ADS indicates adsorption. u indicates the water content in mg/g$_{dry}$
P [Torr]
1000
100
10
1
0,1
0,01
0,001
0,0001
2,75
2,85
2,95
3,05
3,15
3,25
3,35
3,45
3,55
3,65
1000/T [1/K]
(90.5)
(65.8)
(44.3)
(25.4)
(8.5)
t [°C]
= HEAT
= COOL
Water
ADS, u = 135.3
ADS, u = 46.6
ADS, u = 26.7
ADS, u = 16.5
ADS, u = 5.2

Fig. 6a-b.

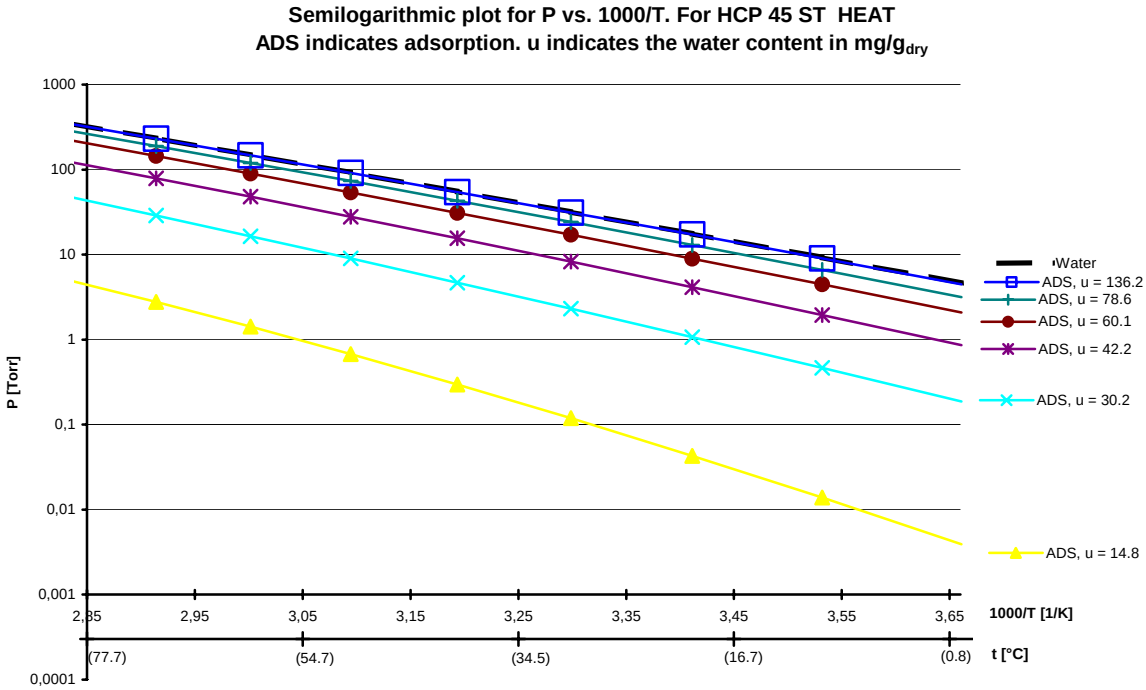
Semilogarithmic plot for P vs. 1000/T. For HCP 45 ST HEAT
ADS indicates adsorption. u indicates the water content in mg/g dry
P [Torr]
1000
100
10
1
0,1
0,01
0,001
0,0001
2,85
2,95
3,05
3,15
3,25
3,35
3,45
3,55
3,65
1000/T [1/K]
(77.7)
(54.7)
(34.5)
(16.7)
(0.8)
t [°C]
Water
ADS, u = 136.2
ADS, u = 78.6
ADS, u = 60.1
ADS, u = 42.2
ADS, u = 30.2
ADS, u = 14.8

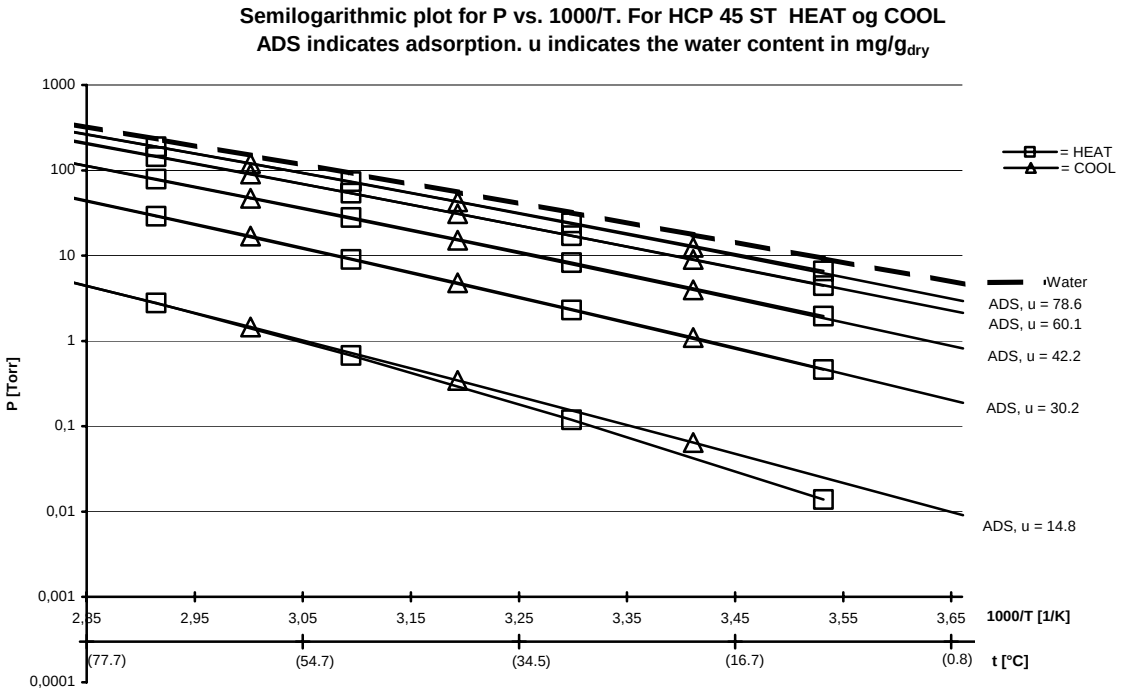
Semilogarithmic plot for P vs. 1000/T. For HCP 45 ST HEAT og COOL
ADS indicates adsorption. u indicates the water content in mg/g dry
P [Torr]
1000
100
10
1
0,1
0,01
0,001
0,0001
2,85
2,95
3,05
3,15
3,25
3,35
3,45
3,55
3,65
1000/T [1/K]
(77.7)
(54.7)
(34.5)
(16.7)
(0.8)
t [°C]
= HEAT
= COOL
Water
ADS, u = 78.6
ADS, u = 60.1
ADS, u = 42.2
ADS, u = 30.2
ADS, u = 14.8

Fig. 7a-b.

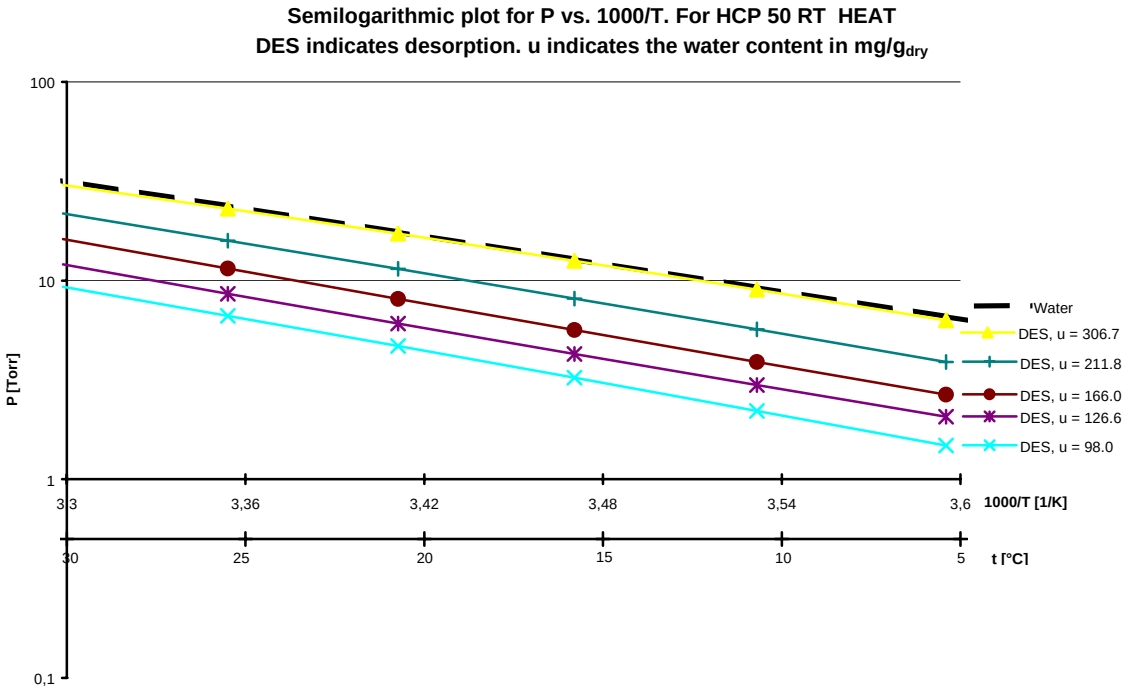
Semilogarithmic plot for P vs. 1000/T. For HCP 50 RT HEAT
DES indicates desorption. u indicates the water content in mg/g dry
100
10
1
0,1
P [Torr]
3,3
3,36
3,42
3,48
3,54
3,6
1000/T [1/K]
30
25
20
15
10
5
t [°C]
'Water
DES, u = 306.7
DES, u = 211.8
DES, u = 166.0
DES, u = 126.6
DES, u = 98.0

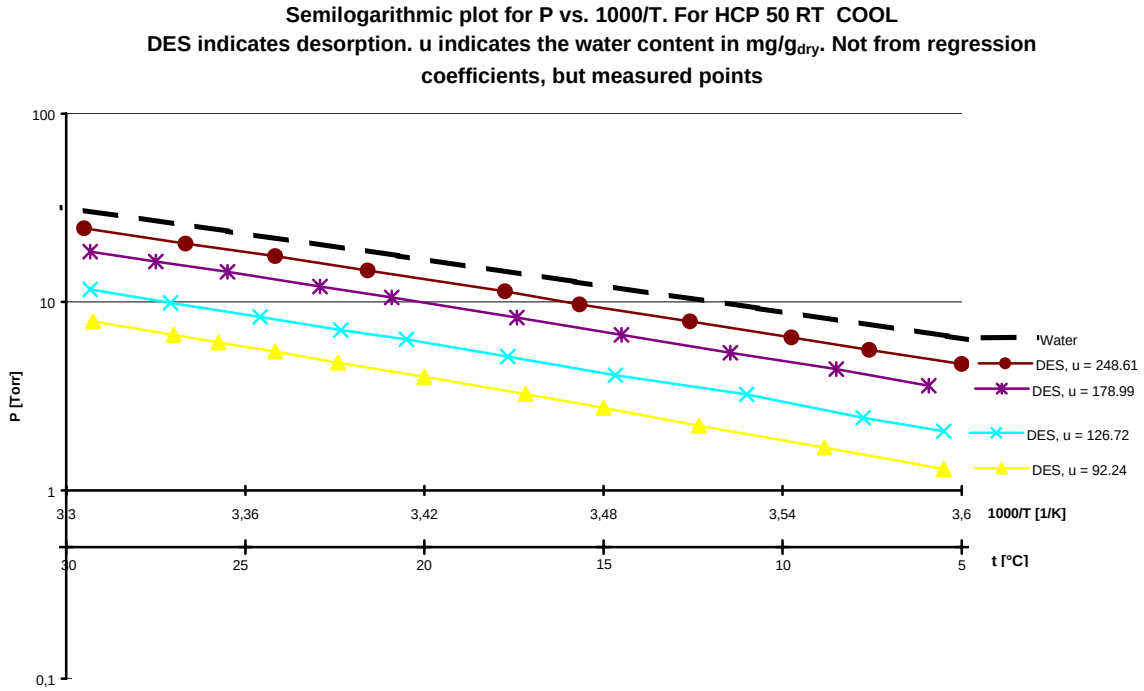
Semilogarithmic plot for P vs. 1000/T. For HCP 50 RT COOL
DES indicates desorption. u indicates the water content in mg/g dry. Not from regression coefficients, but measured points
100
10
1
0,1
P [Torr]
3,3
3,36
3,42
3,48
3,54
3,6
1000/T [1/K]
30
25
20
15
10
5
t [°C]
'Water
DES, u = 248.61
DES, u = 178.99
DES, u = 126.72
DES, u = 92.24

Fig. 8a-b.

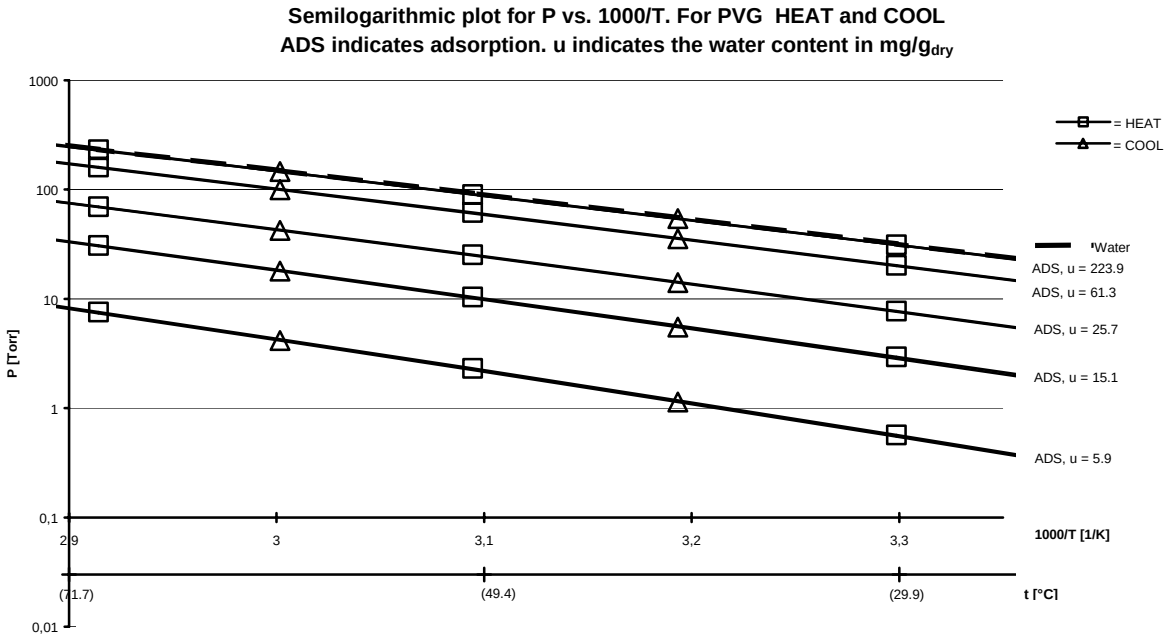
Semilogarithmic plot for P vs. 1000/T. For PVG HEAT and COOL
ADS indicates adsorption. u indicates the water content in mg/g dry
1000
100
10
1
0,1
0,01
P [Torr]
= HEAT
= COOL
Water
ADS, u = 223.9
ADS, u = 61.3
ADS, u = 25.7
ADS, u = 15.1
ADS, u = 5.9
2,9
3
3,1
3,2
3,3
1000/T [1/K]
(71.7)
(49.4)
(29.9)
t [°C]

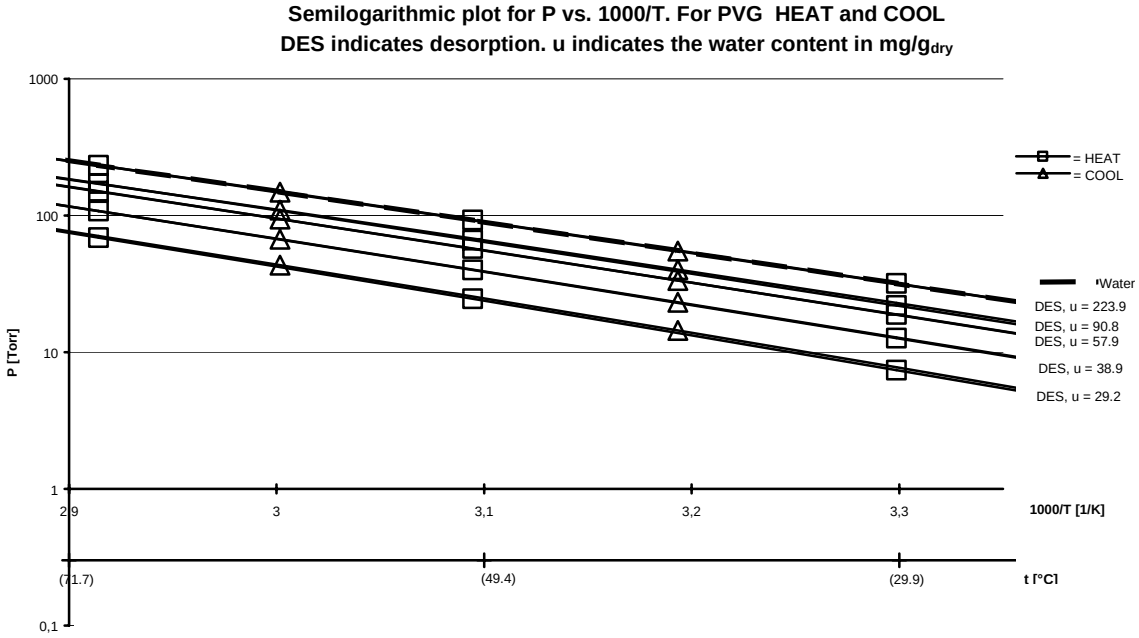
Semilogarithmic plot for P vs. 1000/T. For PVG HEAT and COOL
DES indicates desorption. u indicates the water content in mg/g dry
1000
100
10
1
0,1
P [Torr]
= HEAT
= COOL
Water
DES, u = 223.9
DES, u = 90.8
DES, u = 57.9
DES, u = 38.9
DES, u = 29.2
2,9
3
3,1
3,2
3,3
1000/T [1/K]
(71.7)
(49.4)
(29.9)
t [°C]

Fig. 9.

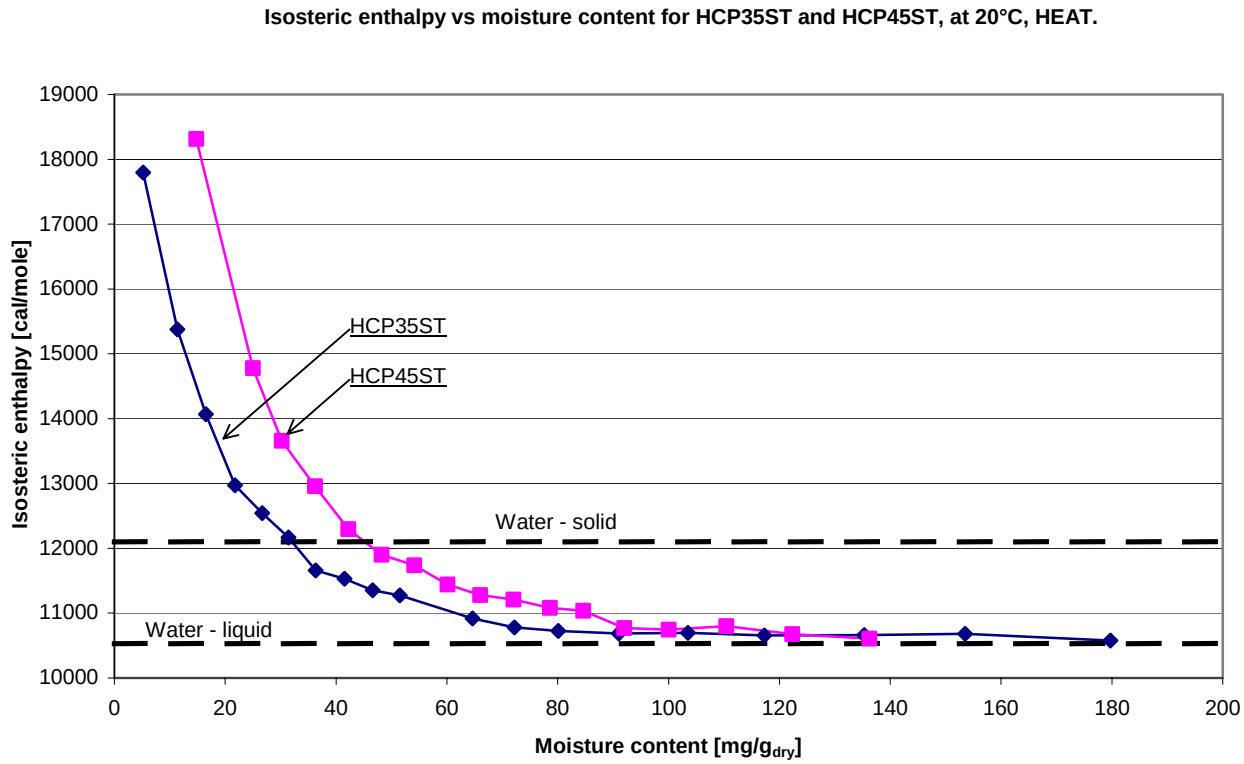
Isosteric enthalpy vs moisture content for HCP35ST and HCP45ST, at 20°C, HEAT.
Isosteric enthalpy [cal/mole]
Moisture content [mg/g$_{dry}$]
HCP35ST
HCP45ST
Water - solid
Water - liquid
19000
18000
17000
16000
15000
14000
13000
12000
11000
10000
0
20
40
60
80
100
120
140
160
180
200

Fig. 10.

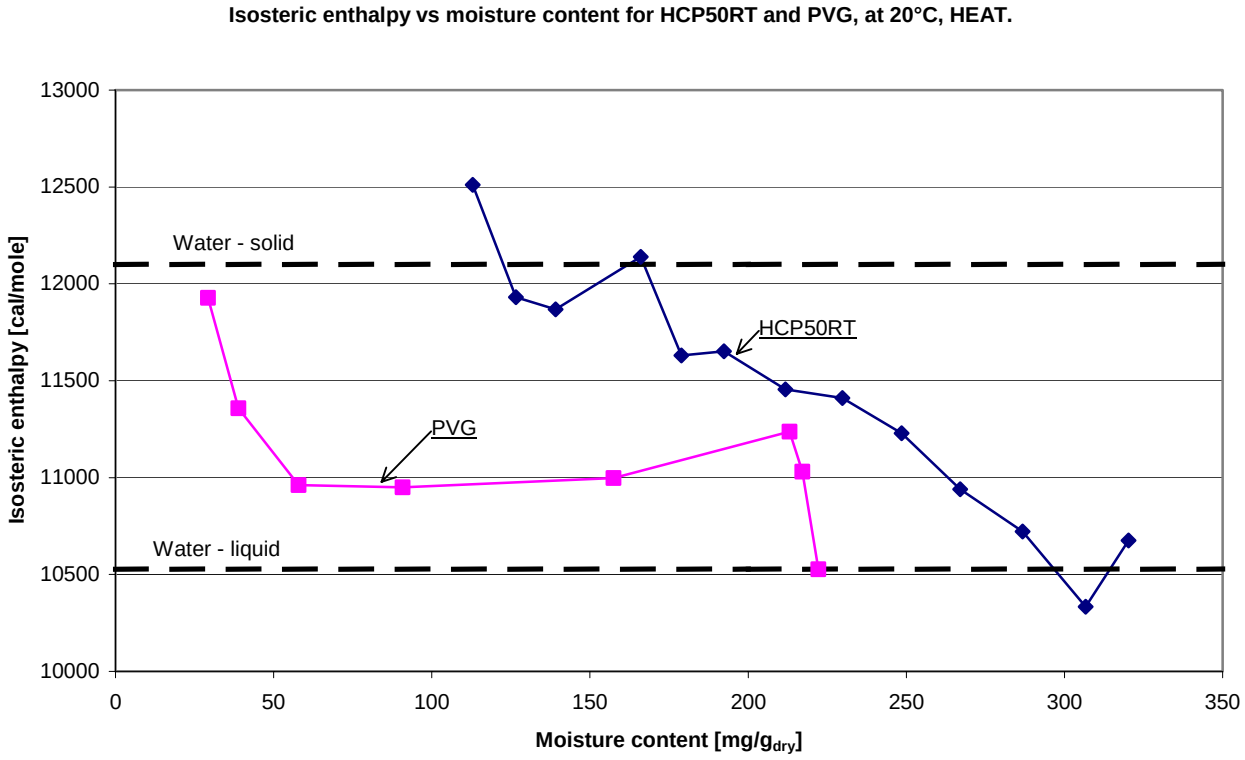
Isosteric enthalpy vs moisture content for HCP50RT and PVG, at 20°C, HEAT.
Isosteric enthalpy [cal/mole]
Moisture content [mg/g$_{dry}$]
Water - solid
Water - liquid
HCP50RT
PVG
13000
12500
12000
11500
11000
10500
10000
0
50
100
150
200
250
300
350

Fig. 11.

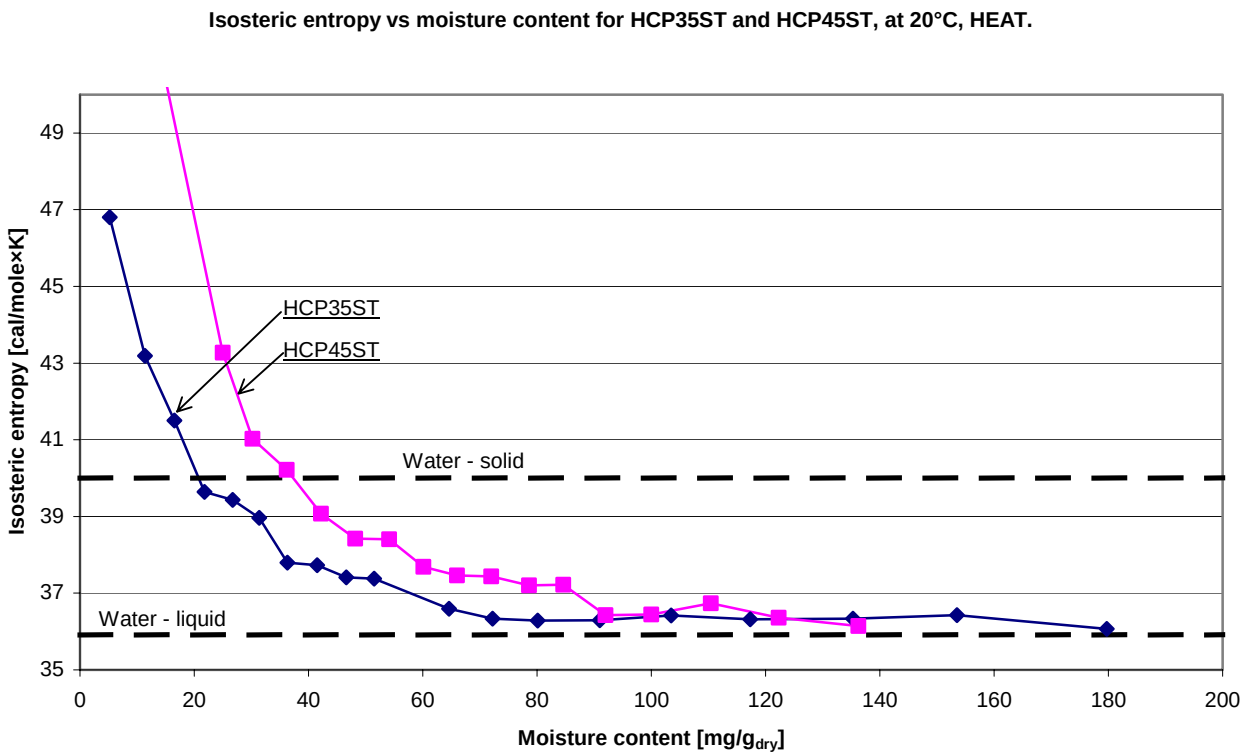
Isosteric entropy vs moisture content for HCP35ST and HCP45ST, at 20°C, HEAT.
Isosteric entropy [cal/mole×K]
49
47
45
43
41
39
37
35
HCP35ST
HCP45ST
Water - solid
Water - liquid
0
20
40
60
80
100
120
140
160
180
200
Moisture content [mg/g$_{dry}$]

Fig. 12.

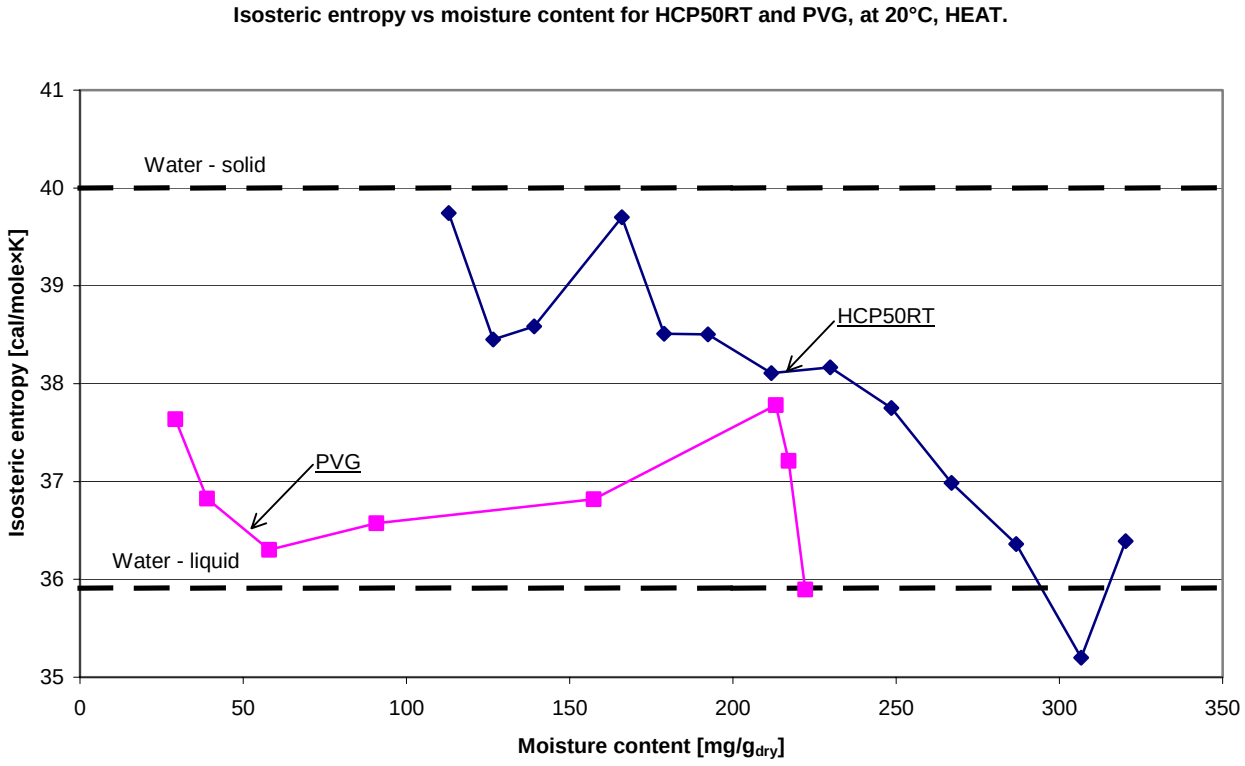
Isosteric entropy vs moisture content for HCP50RT and PVG, at 20°C, HEAT.
Isosteric entropy [cal/mole×K]
41
40
39
38
37
36
35
Water - solid
HCP50RT
PVG
Water - liquid
0
50
100
150
200
250
300
350
Moisture content [mg/g$_{dry}$]

Fig. 13a-b.

Isosteric enthalpy vs relative vapor pressure for all materials, Adsorption, at 20°C, HEAT.

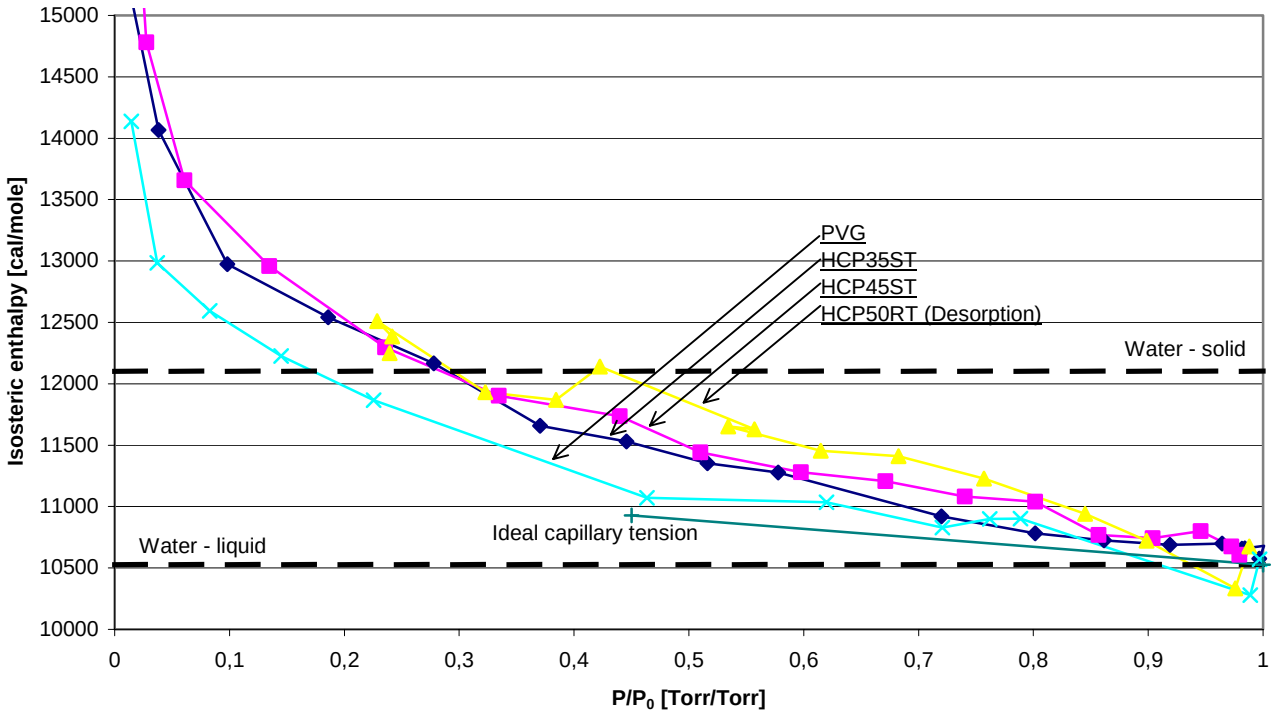

Isosteric enthalpy vs relative vapor pressure for all materials, Adsorption, at 20°C, HEAT.
Smoothed curves from Fig. 13a.

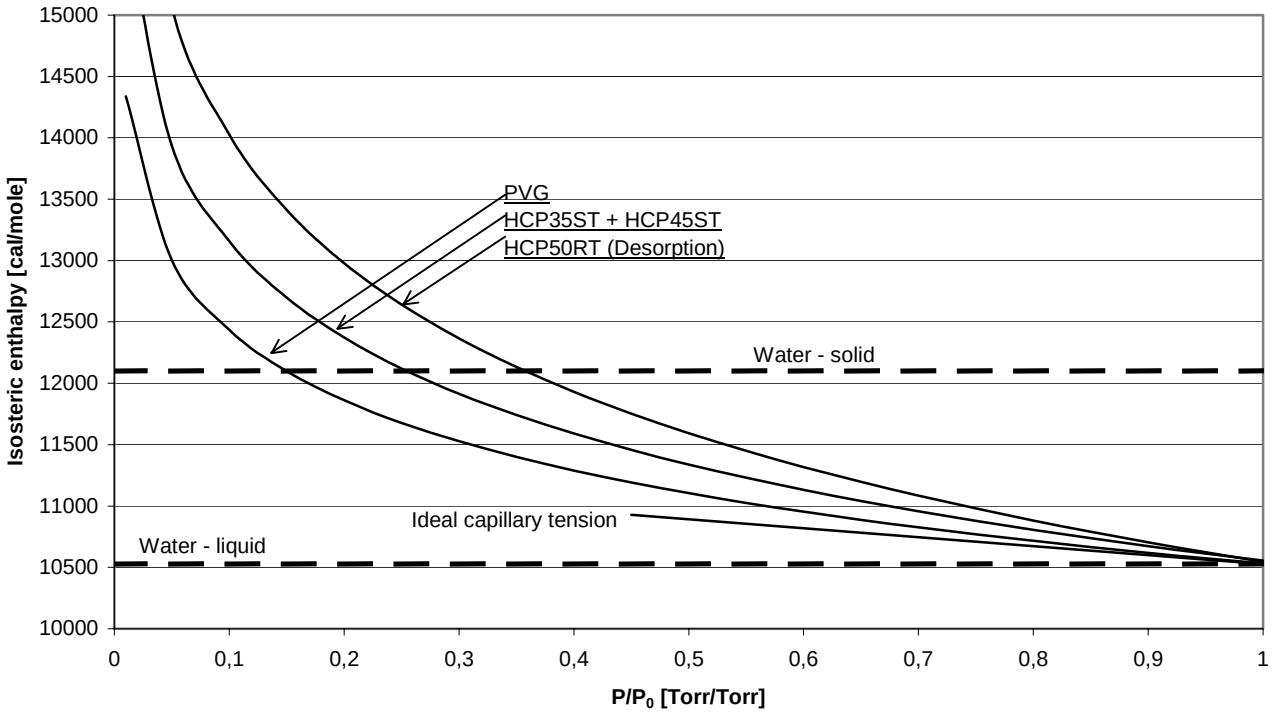

Fig. 13c-d.

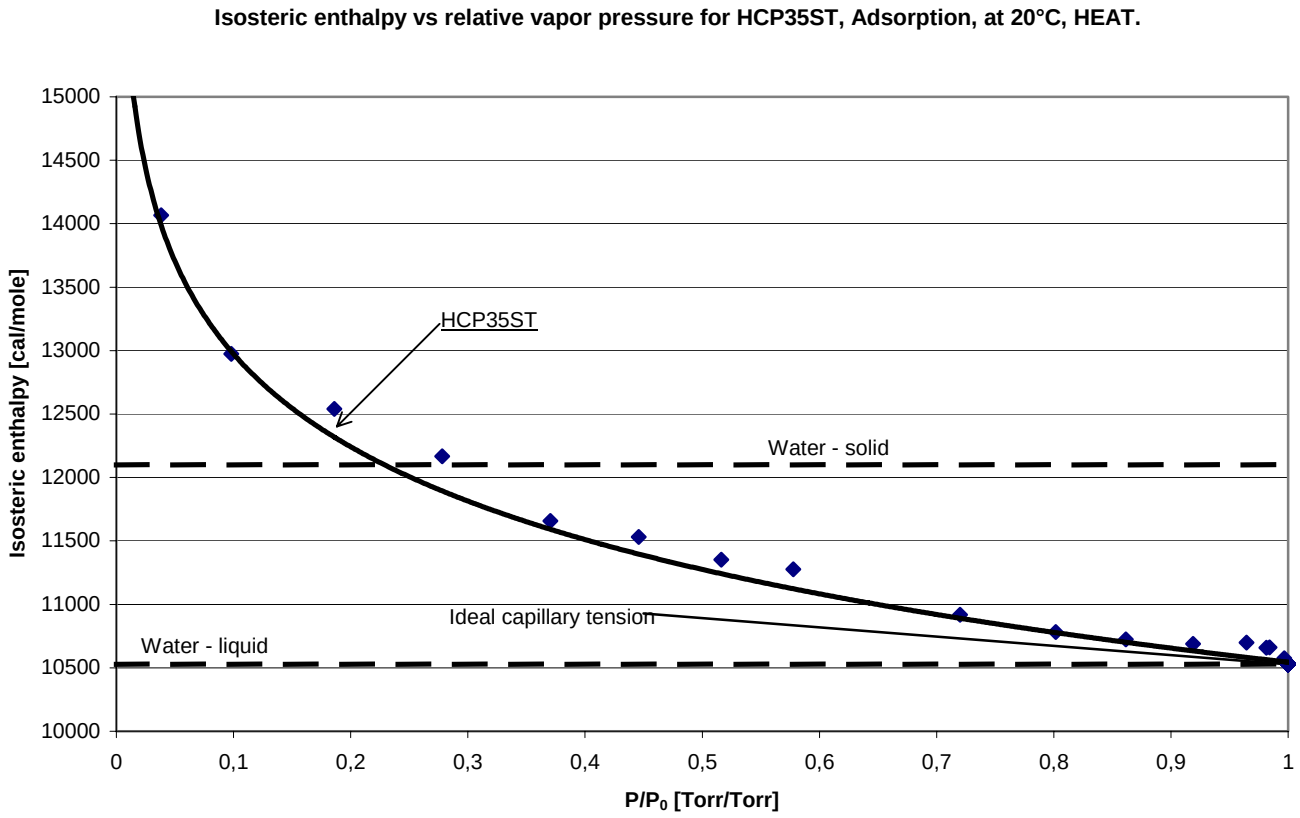
Isosteric enthalpy vs relative vapor pressure for HCP35ST, Adsorption, at 20°C, HEAT.
Isosteric enthalpy [cal/mole]
15000
14500
14000
13500
13000
12500
12000
11500
11000
10500
10000
HCP35ST
Water - solid
Ideal capillary tension
Water - liquid
0
0,1
0,2
0,3
0,4
0,5
0,6
0,7
0,8
0,9
1
P/P0 [Torr/Torr]

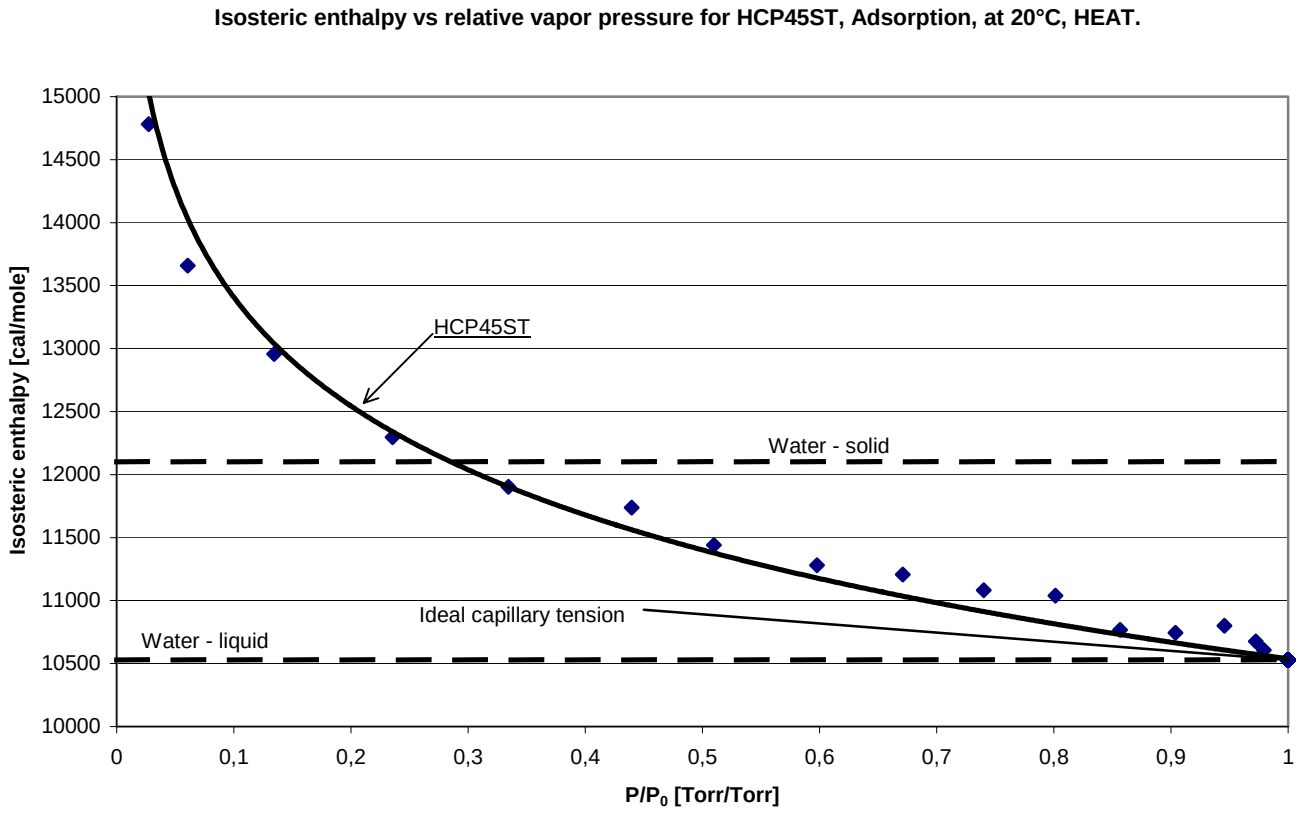
Isosteric enthalpy vs relative vapor pressure for HCP45ST, Adsorption, at 20°C, HEAT.
Isosteric enthalpy [cal/mole]
15000
14500
14000
13500
13000
12500
12000
11500
11000
10500
10000
HCP45ST
Water - solid
Ideal capillary tension
Water - liquid
0
0,1
0,2
0,3
0,4
0,5
0,6
0,7
0,8
0,9
1
P/P0 [Torr/Torr]

Fig. 13e-f.

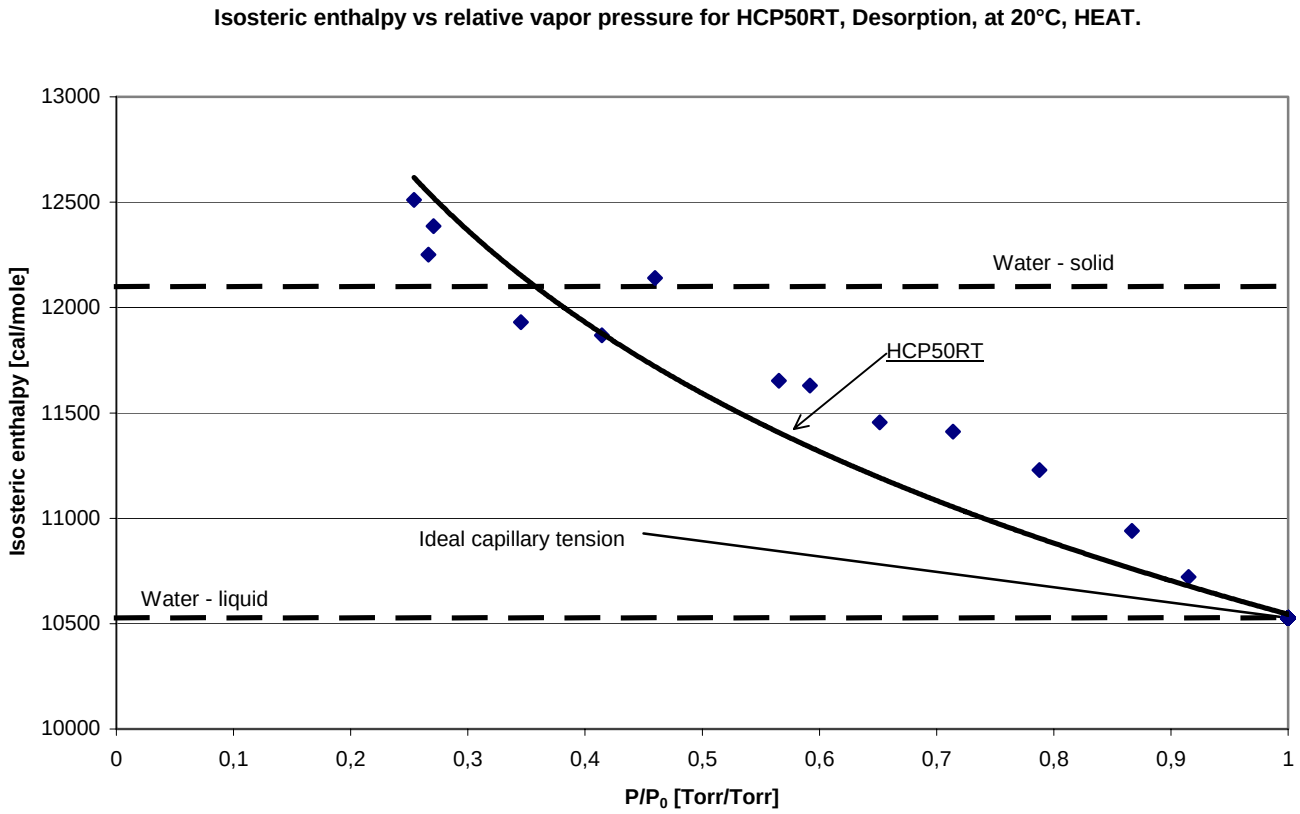
Isosteric enthalpy vs relative vapor pressure for HCP50RT, Desorption, at 20°C, HEAT.
Isosteric enthalpy [cal/mole]
13000
12500
12000
11500
11000
10500
10000
Water - solid
HCP50RT
Ideal capillary tension
Water - liquid
0
0,1
0,2
0,3
0,4
0,5
0,6
0,7
0,8
0,9
1
P/P0 [Torr/Torr]

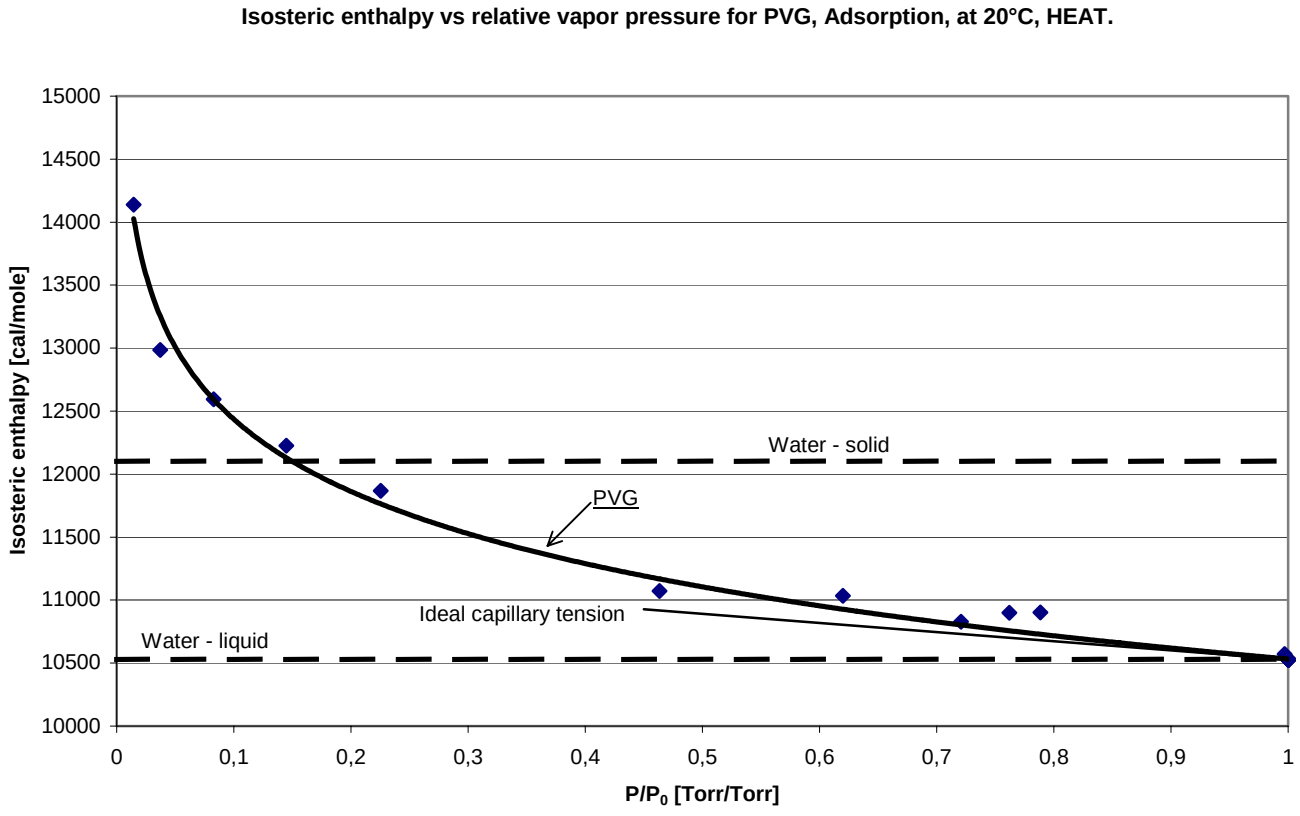
Isosteric enthalpy vs relative vapor pressure for PVG, Adsorption, at 20°C, HEAT.
Isosteric enthalpy [cal/mole]
15000
14500
14000
13500
13000
12500
12000
11500
11000
10500
10000
Water - solid
PVG
Ideal capillary tension
Water - liquid
0
0,1
0,2
0,3
0,4
0,5
0,6
0,7
0,8
0,9
1
P/P0 [Torr/Torr]

Fig. 14a-b.

Isosteric entropy vs relative vapor presure for all materials, Adsorption, at 20°C, HEAT.

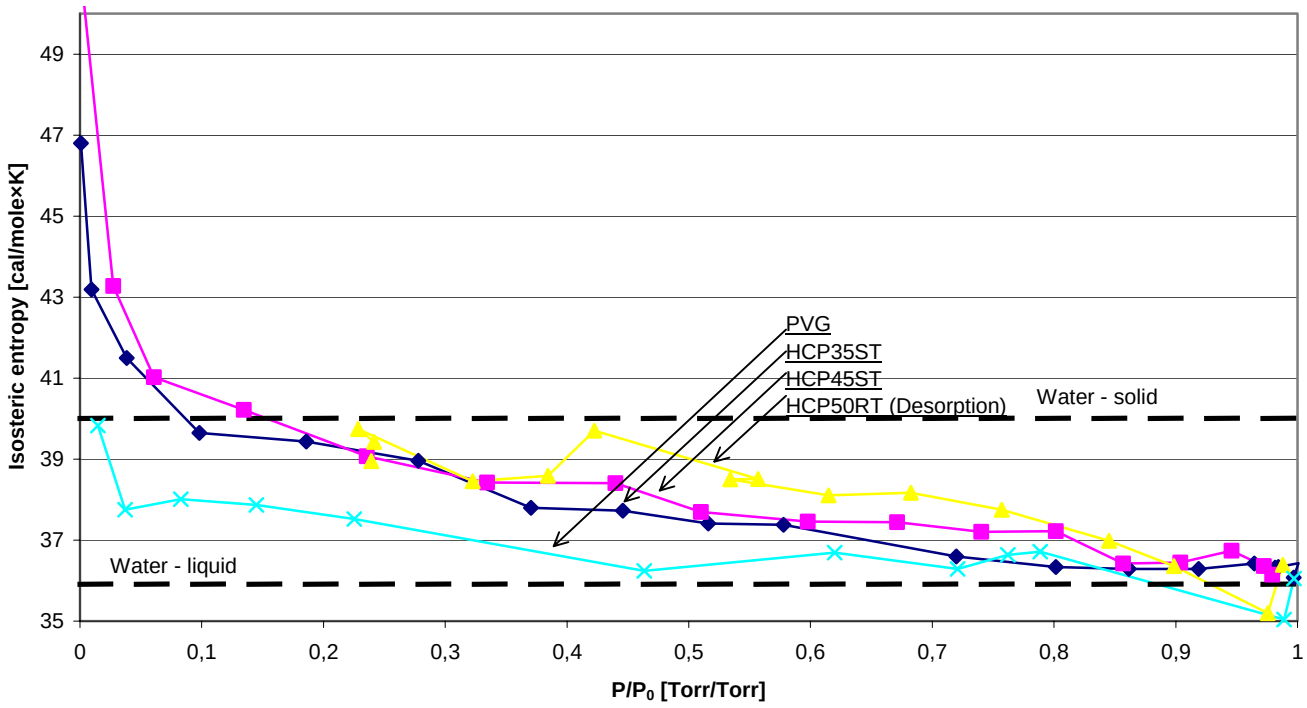

Isosteric entropy vs relative vapor presure for all materials, Adsorption, at 20°C, HEAT.
Smoothed curves from Fig. 14a.

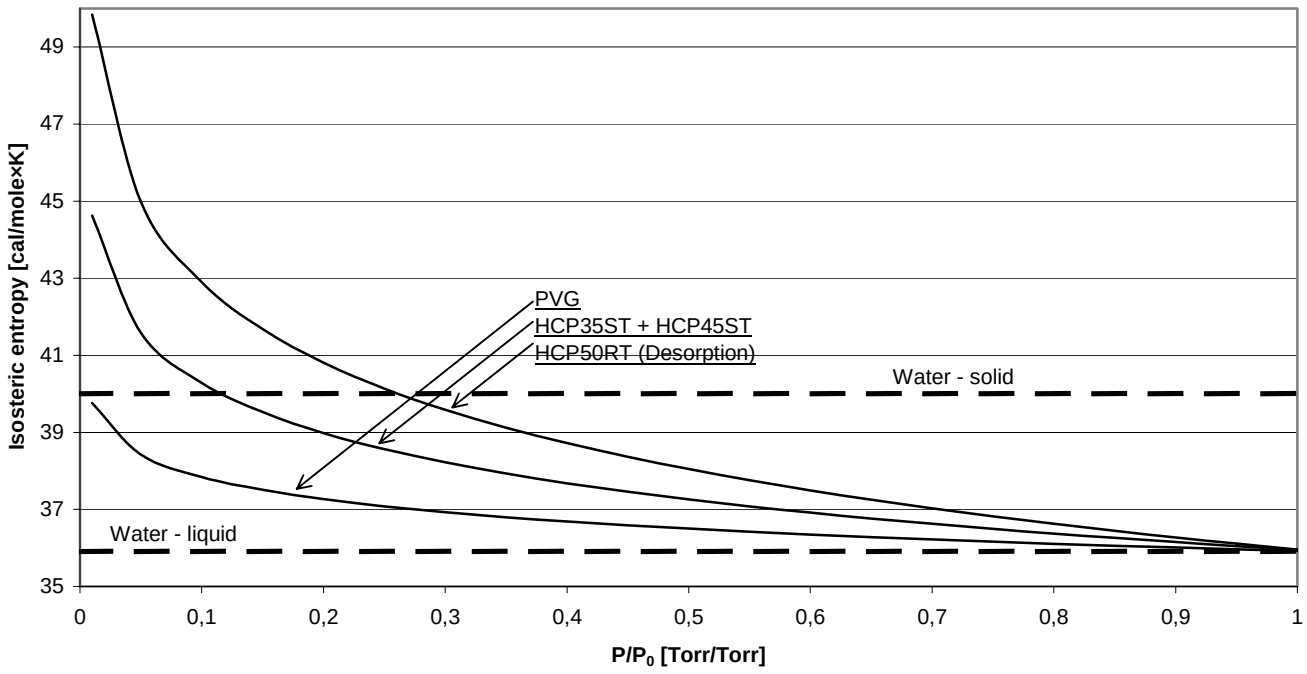

Fig. 14c-d.

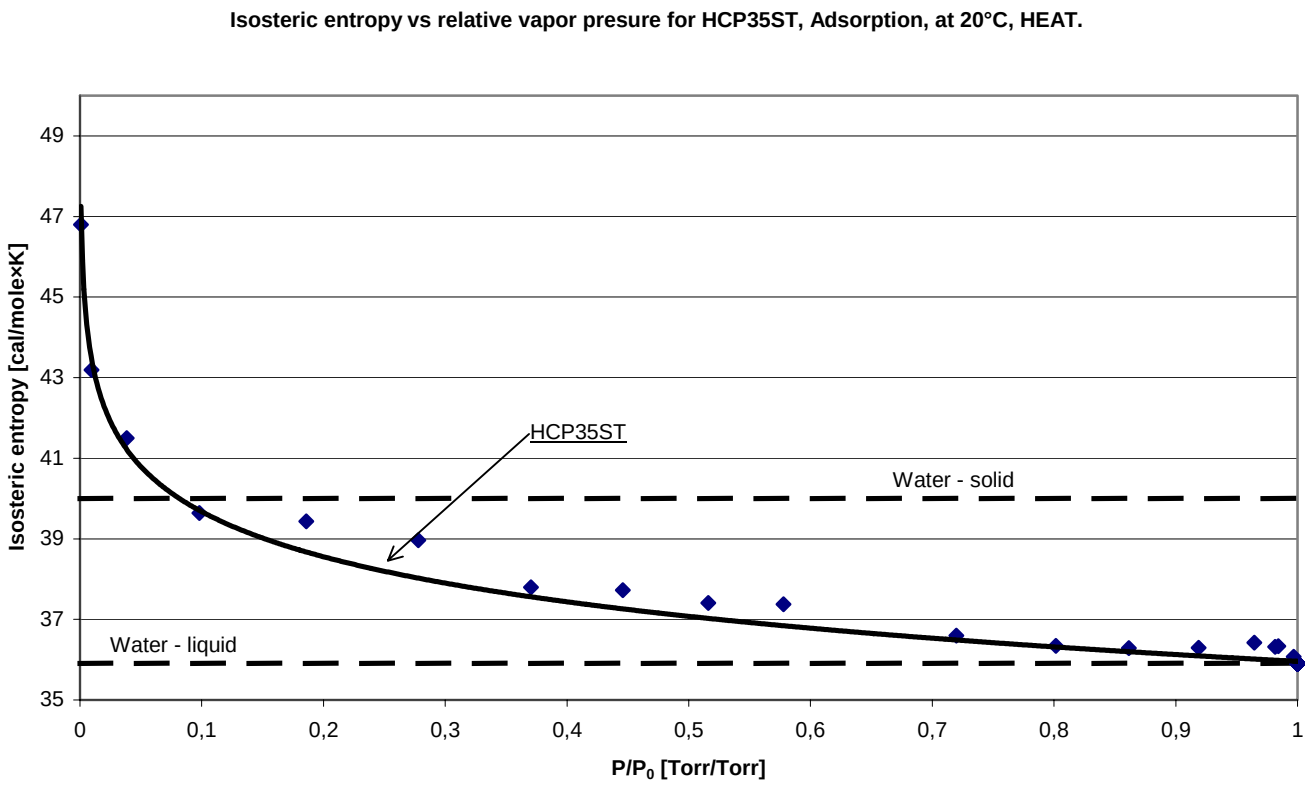
Isosteric entropy vs relative vapor presure for HCP35ST, Adsorption, at 20°C, HEAT.
Isosteric entropy [cal/mole×K]
49
47
45
43
41
39
37
35
HCP35ST
Water - solid
Water - liquid
0
0,1
0,2
0,3
0,4
0,5
0,6
0,7
0,8
0,9
1
P/P0 [Torr/Torr]

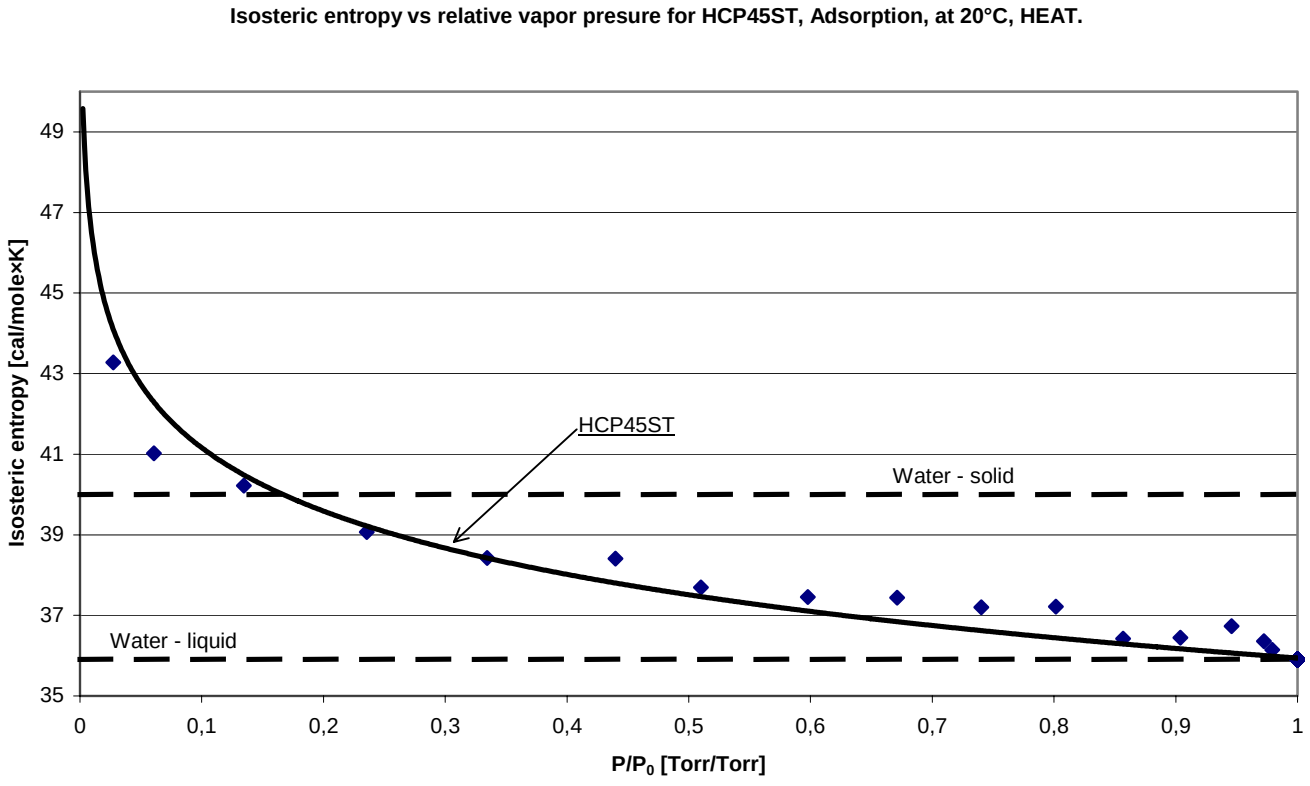
Isosteric entropy vs relative vapor presure for HCP45ST, Adsorption, at 20°C, HEAT.
Isosteric entropy [cal/mole×K]
49
47
45
43
41
39
37
35
HCP45ST
Water - solid
Water - liquid
0
0,1
0,2
0,3
0,4
0,5
0,6
0,7
0,8
0,9
1
P/P0 [Torr/Torr]

Fig. 14e-f.

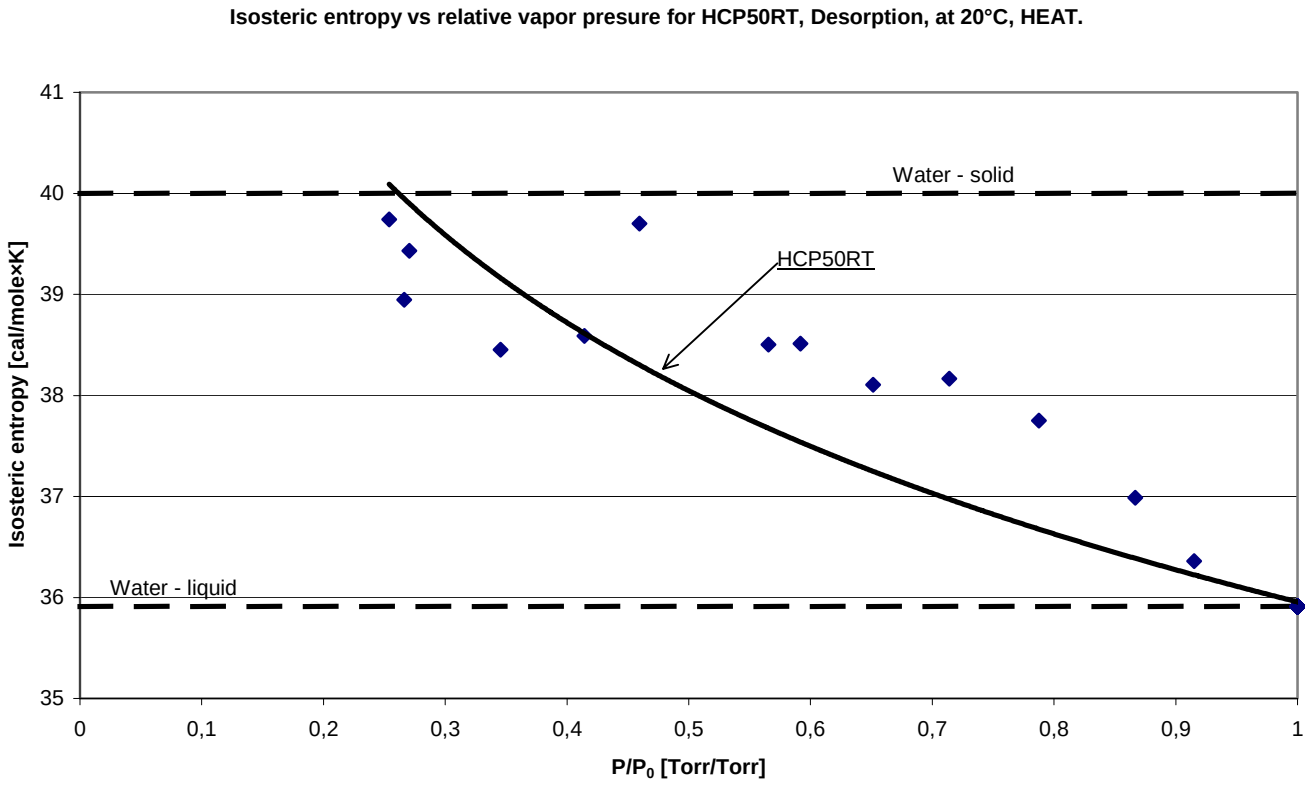
Isosteric entropy vs relative vapor presure for HCP50RT, Desorption, at 20°C, HEAT.
Isosteric entropy [cal/mole×K]
41
40
39
38
37
36
35
Water - solid
HCP50RT
Water - liquid
0
0,1
0,2
0,3
0,4
0,5
0,6
0,7
0,8
0,9
1
P/P0 [Torr/Torr]

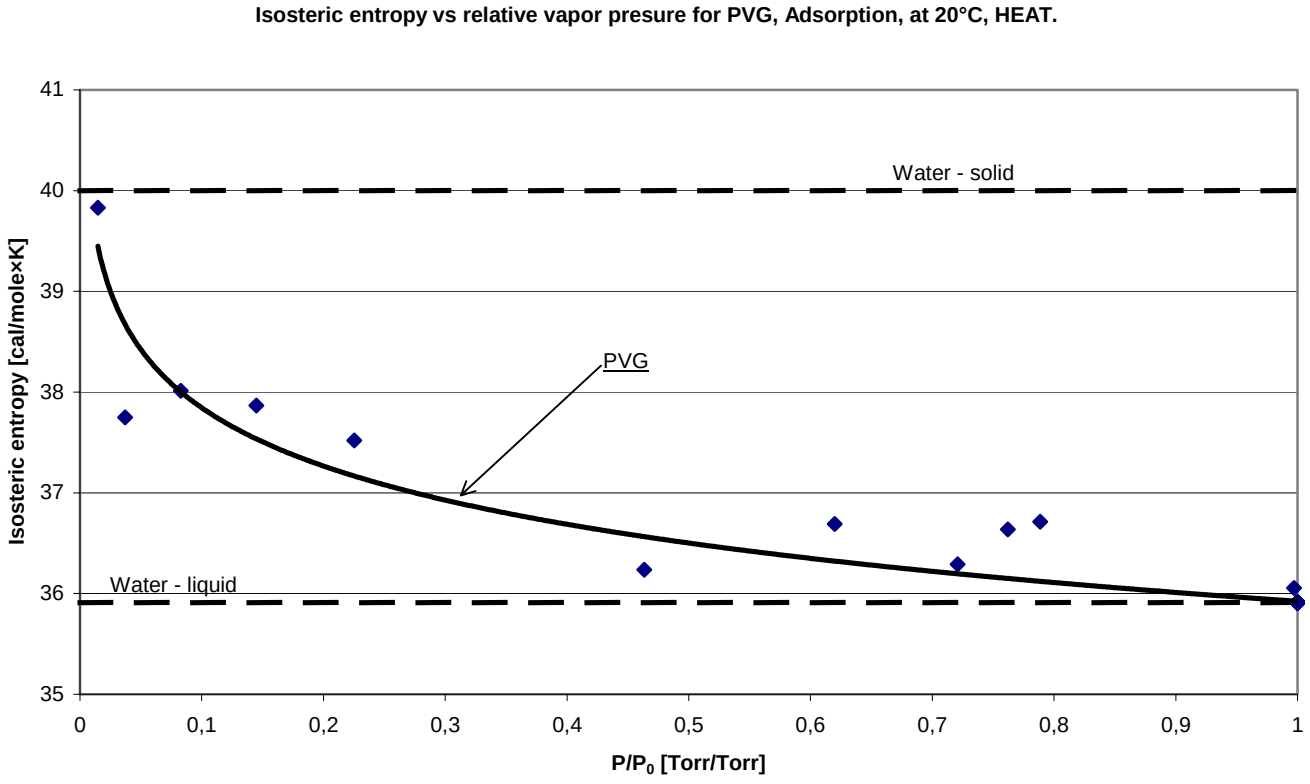
Isosteric entropy vs relative vapor presure for PVG, Adsorption, at 20°C, HEAT.
Isosteric entropy [cal/mole×K]
41
40
39
38
37
36
35
Water - solid
PVG
Water - liquid
0
0,1
0,2
0,3
0,4
0,5
0,6
0,7
0,8
0,9
1
P/P0 [Torr/Torr]

Fig. 15a-b.

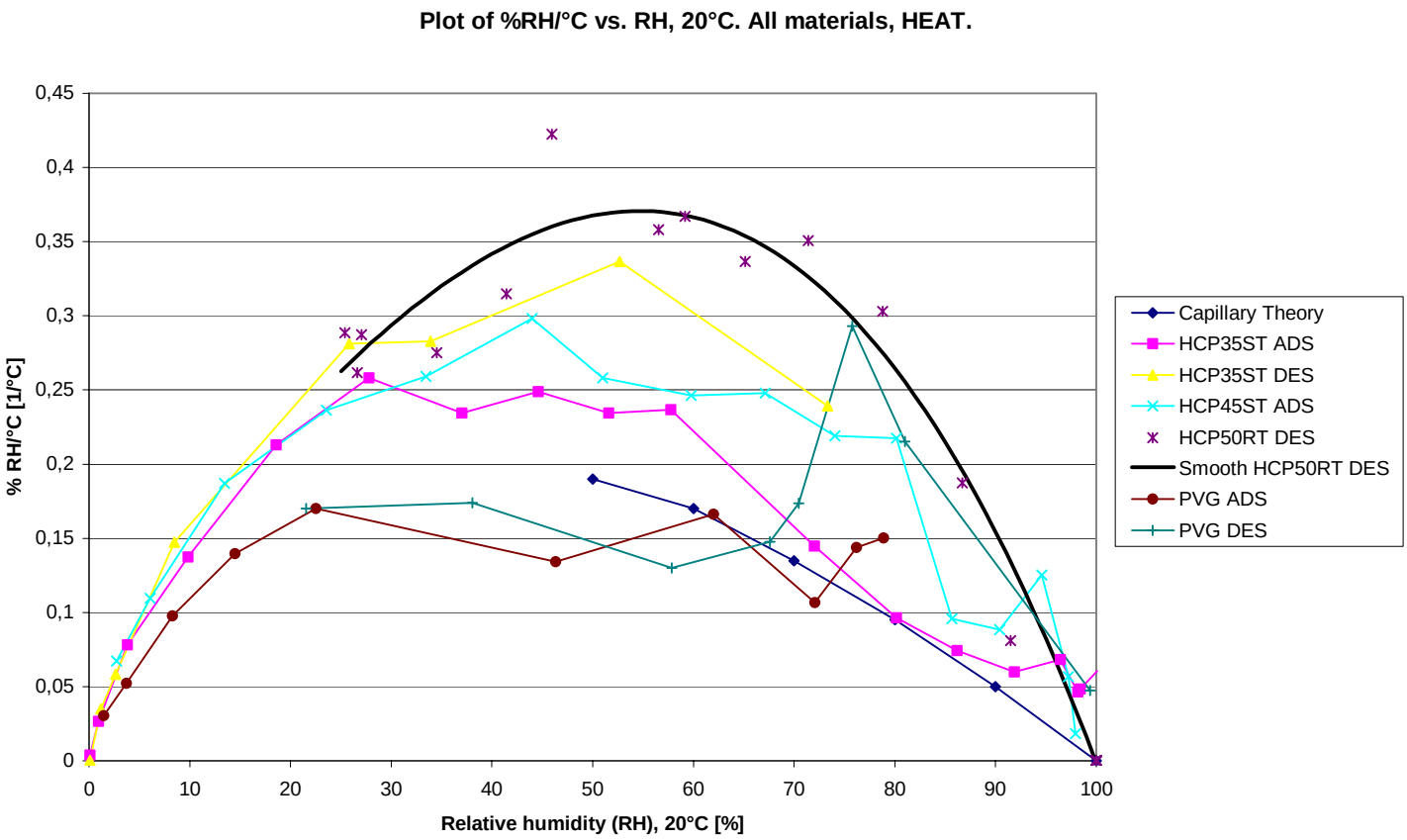
Plot of %RH/°C vs. RH, 20°C. All materials, HEAT.
% RH/°C [1/°C]
Relative humidity (RH), 20°C [%]
Capillary Theory
HCP35ST ADS
HCP35ST DES
HCP45ST ADS
HCP50RT DES
Smooth HCP50RT DES
PVG ADS
PVG DES

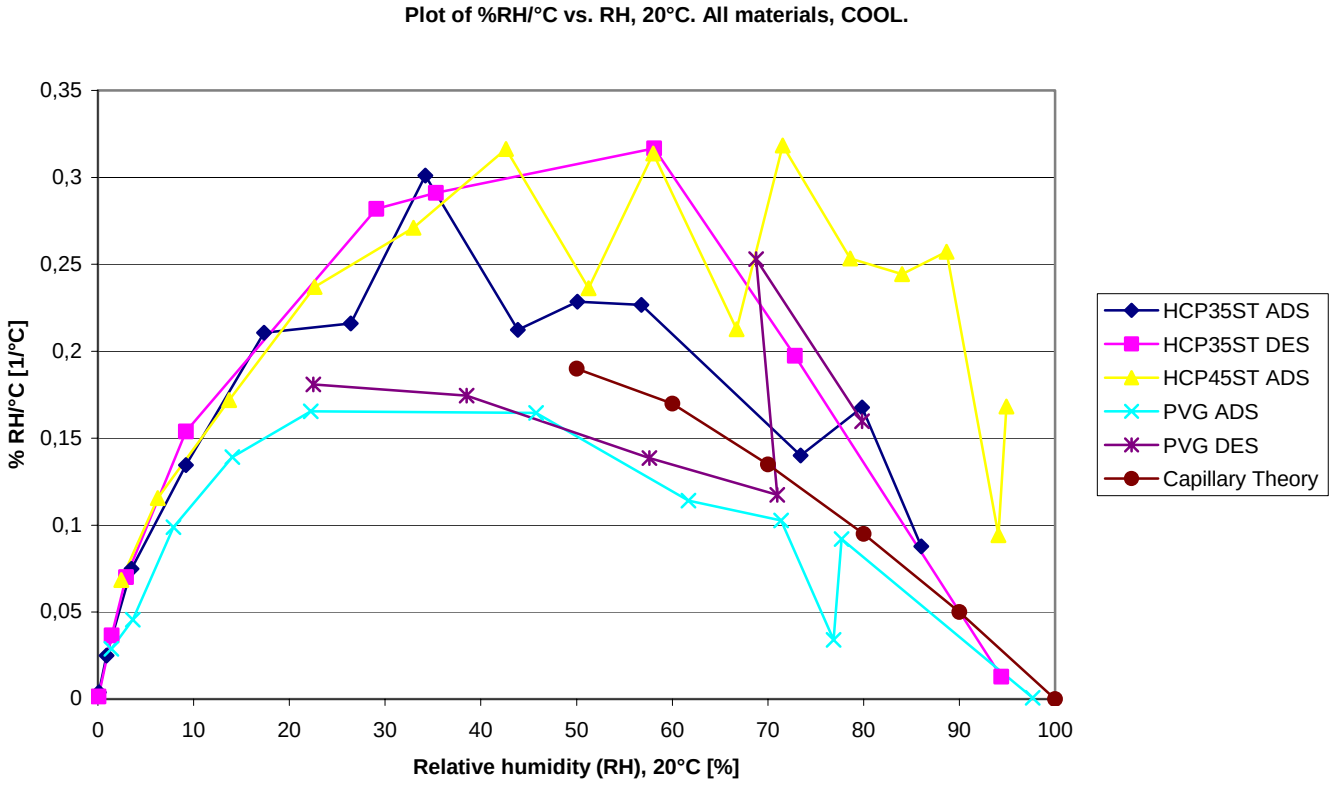
Plot of %RH/°C vs. RH, 20°C. All materials, COOL.
% RH/°C [1/°C]
Relative humidity (RH), 20°C [%]
HCP35ST ADS
HCP35ST DES
HCP45ST ADS
PVG ADS
PVG DES
Capillary Theory

Fig. 15c.

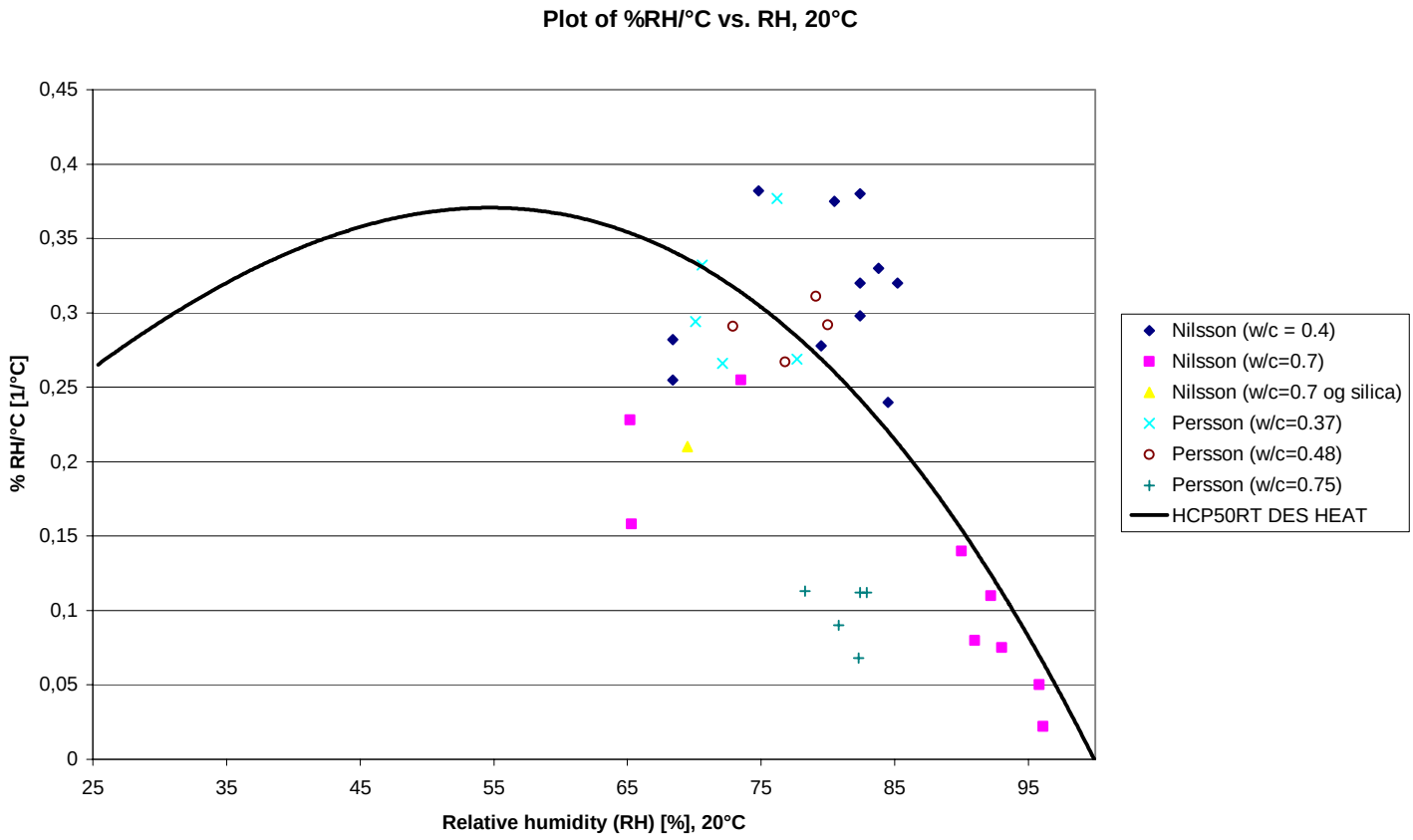
Plot of %RH/°C vs. RH, 20°C
% RH/°C [1/°C]
0,45
0,4
0,35
0,3
0,25
0,2
0,15
0,1
0,05
0
25
35
45
55
65
75
85
95
Relative humidity (RH) [%], 20°C
Nilsson (w/c = 0.4)
Nilsson (w/c=0.7)
Nilsson (w/c=0.7 og silica)
Persson (w/c=0.37)
Persson (w/c=0.48)
Persson (w/c=0.75)
HCP50RT DES HEAT

Fig. 16a-b.

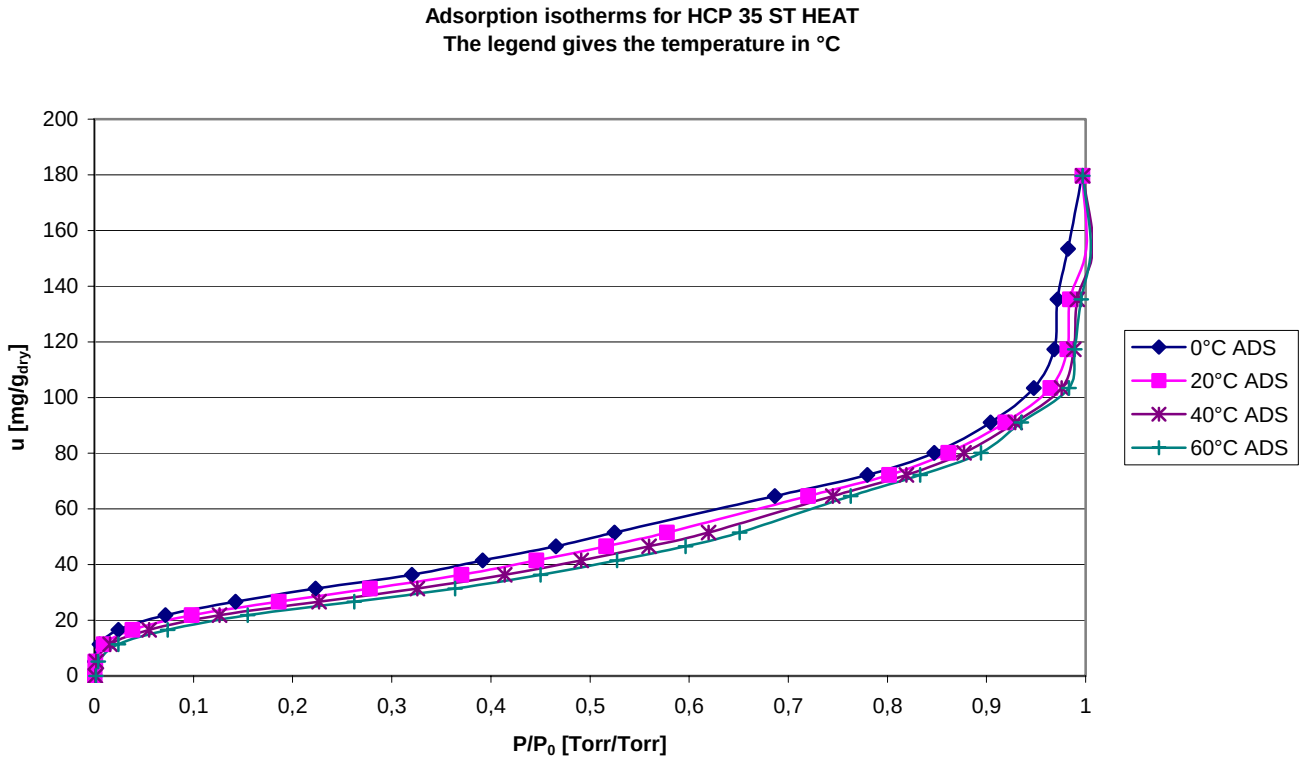
Adsorption isotherms for HCP 35 ST HEAT
The legend gives the temperature in °C
u [mg/g$_{dry}$]
P/P$_0$ [Torr/Torr]
0°C ADS
20°C ADS
40°C ADS
60°C ADS

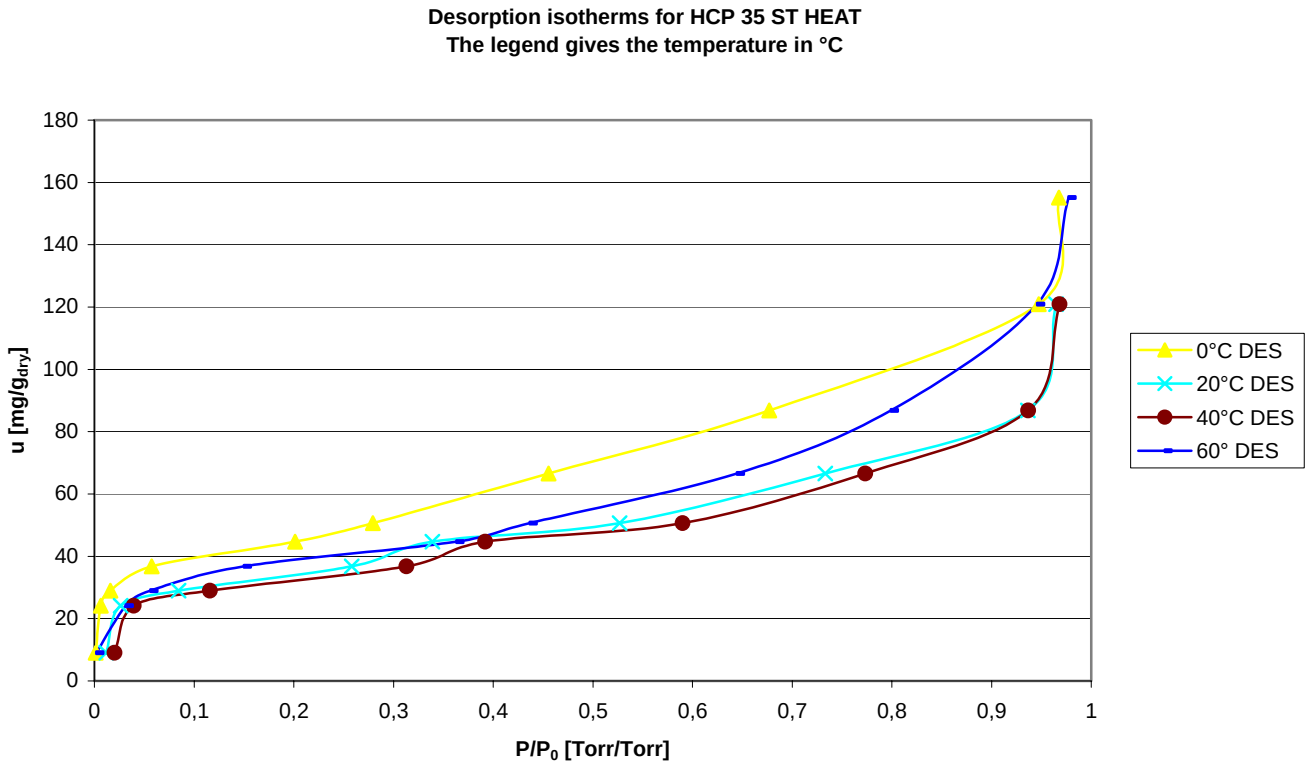
Desorption isotherms for HCP 35 ST HEAT
The legend gives the temperature in °C
u [mg/g$_{dry}$]
P/P$_0$ [Torr/Torr]
0°C DES
20°C DES
40°C DES
60° DES

Fig. 17.

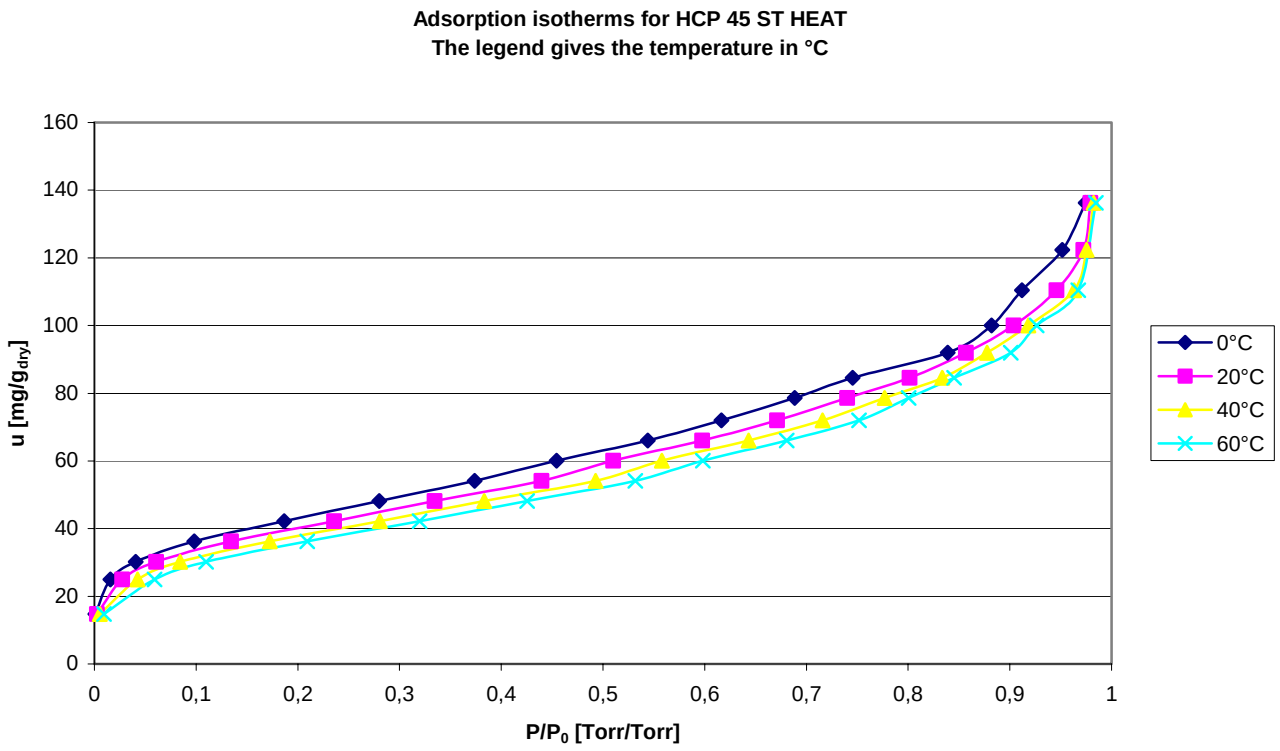
Adsorption isotherms for HCP 45 ST HEAT
The legend gives the temperature in °C
u [mg/g$_{dry}$]
160
140
120
100
80
60
40
20
0
0
0,1
0,2
0,3
0,4
0,5
0,6
0,7
0,8
0,9
1
P/P$_0$ [Torr/Torr]
0°C
20°C
40°C
60°C

Fig. 18.

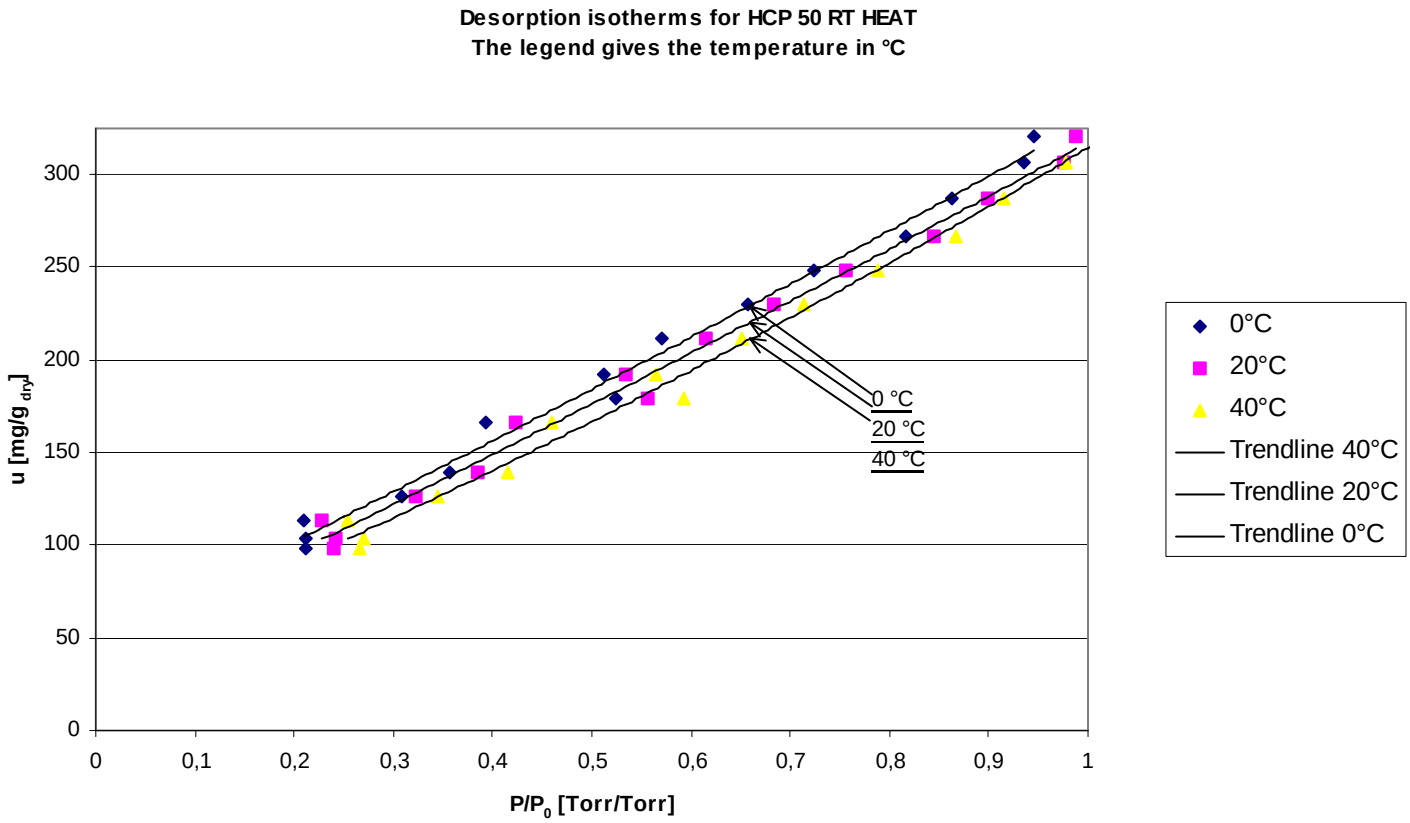
Desorption isotherms for HCP 50 RT HEAT
The legend gives the temperature in °C
u [mg/g dry]
P/P0 [Torr/Torr]
0
50
100
150
200
250
300
0
0,1
0,2
0,3
0,4
0,5
0,6
0,7
0,8
0,9
1
0 °C
20 °C
40 °C
0°C
20°C
40°C
Trendline 40°C
Trendline 20°C
Trendline 0°C

Fig. 19a-b.

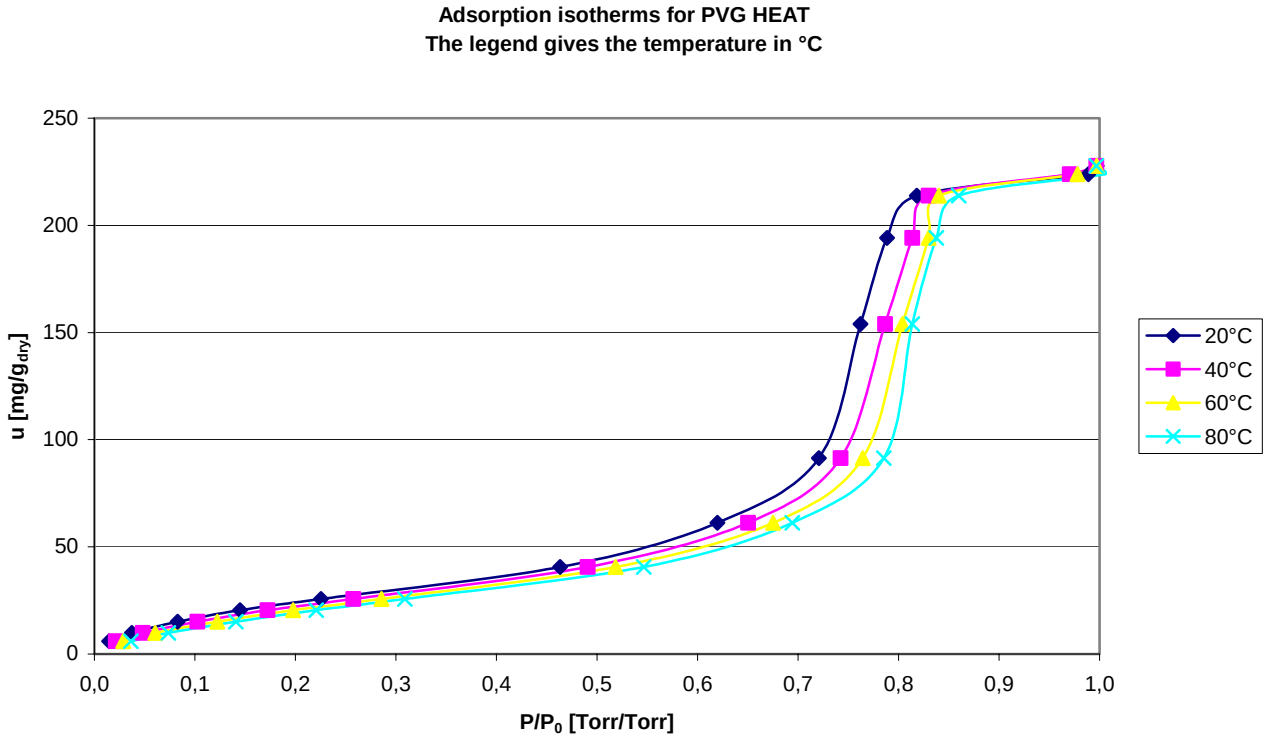
Adsorption isotherms for PVG HEAT
The legend gives the temperature in °C
u [mg/g$_{dry}$]
P/P$_0$ [Torr/Torr]
20°C
40°C
60°C
80°C

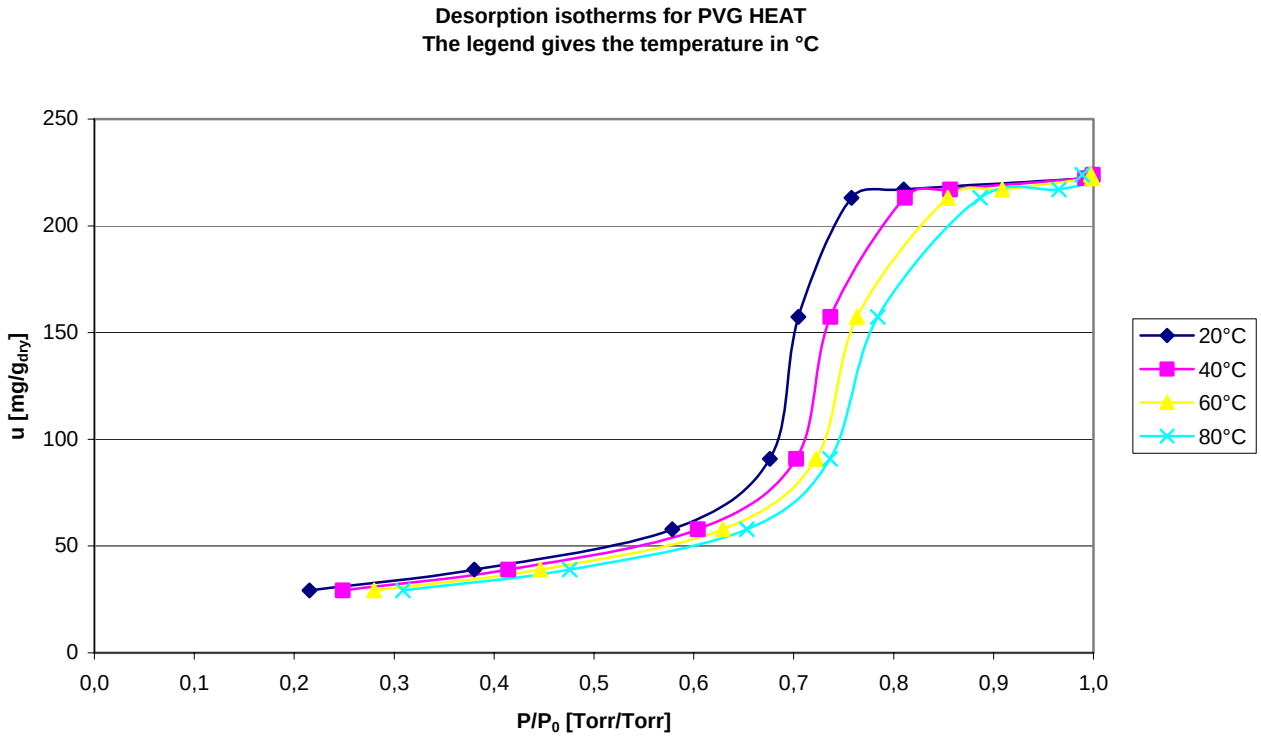
Desorption isotherms for PVG HEAT
The legend gives the temperature in °C
u [mg/g$_{dry}$]
P/P$_0$ [Torr/Torr]
20°C
40°C
60°C
80°C